Running Head: Transplanting ESC-derived rods via surface markers

Title: Transplantation of photoreceptor precursors isolated via a cell surface biomarker panel from embryonic stem cell-derived self-forming retina

Authors: Jorn Lakowski[1], Anai Gonzalez-Cordero[2], Emma L. West[2], Ya-Ting Han[1], Emily Welby[1], Arifa Naeem[2], Samuel J I Blackford[2], James W. B. Bainbridge[2], Rachael A. Pearson[2], Robin R. Ali[2], Jane C. Sowden*[1]

Address: [1] Stem Cells and Regenerative Medicine Section, UCL Institute of Child Health, University College London, 30 Guilford Street, London, WC1N 1EH UK

[2] Department of Genetics, UCL Institute of Ophthalmology, 11-43 Bath Street, London, EC1V 9EL UK

Author Contributions:

Jorn Lakowski: Conception and design, collection and/or assembly of data, data analysis and interpretation, manuscript writing, financial support.

Anai Gonzalez-Cordero: Conception and design, collection and/or assembly of data, data analysis and interpretation, manuscript writing.

Emma West: Conception and design, collection and/or assembly of data, data analysis and interpretation.

Ya-Ting Han: Collection and/or assembly of data, manuscript writing.

Emily Welby: Collection and/or assembly of data.

Arifa Naeem: Collection and/or assembly of data.

Samuel J I Blackford: Collection and/or assembly of data.

James W. B. Bainbridge: Collection and/or assembly of data.

Rachael A Pearson: Conception and design, collection and/or assembly of data, manuscript writing, financial support.

Robin R Ali: Conception and design, manuscript writing, financial support.

Jane C Sowden: Conception and design, data analysis and interpretation, manuscript writing, final approval of manuscript, financial support.

*__Correspondence to__: Professor Jane C. Sowden, PhD: j.sowden@ucl.ac.uk or Dr Jorn Lakowski, PhD (j.lakowski@ucl.ac.uk), Stem Cells and Regenerative Medicine Section, UCL Institute of Child Health, University College London, 30 Guilford Street, London, WC1N 1EH UK, UK, Tel: +44 (0) 20 7905 2121, Fax: +44 (0) 20 7831 4366

Key Words: Photoreceptor cells, retina, surface antigens, blindness, retinal dystrophies, embryonic stem cells, transplantation

Abstract

Loss of photoreceptors due to retinal degeneration is a major cause of untreatable blindness. Cell replacement therapy, using pluripotent stem cell-derived photoreceptor cells, may be a feasible future treatment. Achieving safe and effective cell replacement is critically dependent on the stringent selection and purification of optimal cells for transplantation. Previously, we demonstrated effective transplantation of post-mitotic photoreceptor precursor cells labeled by fluorescent reporter genes. As genetically-labeled cells are not desirable for therapy, here we developed a surface biomarker cell selection strategy for application to complex pluripotent stem cell differentiation cultures. We show that a five cell surface biomarker panel CD73(+)CD24(+)CD133(+)CD47(+)CD15(-) facilitates the isolation of photoreceptor precursors from 3D self-forming retina differentiated from mouse embryonic stem cells. Importantly, stem cell-derived cells isolated using the biomarker panel successfully integrate and mature into new rod photoreceptors in the adult mouse retinae after subretinal transplantation. Conversely, unsorted or negatively selected cells do not give rise to newly integrated rods after transplantation. The biomarker panel also removes detrimental proliferating cells prior to transplantation. Notably, we demonstrate how expression of the biomarker panel is conserved in the human retina and propose that a similar selection strategy will facilitate isolation of human transplantation-competent cells for therapeutic application.

Introduction

Many retinopathies, while variable in their aetiology, share a common end point, the loss of rod and cone photoreceptors in the retina [1]. Inherited retinal degenerations arise from mutations in one of more than 200 different genes [2]. In the majority of cases rod photoreceptors are affected first while loss of cone photoreceptors is secondary due to a trophic dependence on the adjacent rods [3]. Worldwide the number of people blinded by retinal degenerative conditions, including age related macular degeneration is estimated to be more than 3.2 million and is predicted to rise as life expectancy increases [4, 5]. Unfortunately, the human retina lacks any significant regenerative potential to replace lost photoreceptors; consequently once these cells have degenerated the resulting visual impairment is permanent. These conditions present a high socio-economic burden for patients, their families, and the healthcare system [6]. While significant progress has been achieved over the past decade in understanding the underlying molecular mechanisms for a range of retinal diseases, current treatment options only delay the onset or decelerate the condition.

To address the current lack of effective treatments much research effort has been focused on the development of novel therapeutic strategies. Cell replacement therapy, the reintroduction of healthy photoreceptors into the degenerating retina, constitutes such an approach. We and others have previously shown that post-mitotic, yet immature photoreceptor precursors, derived from a defined time window during postnatal development in the mouse can integrate into the existing retinal architecture of the normal and diseased adult retina [7-14] and contribute to the retinotopic map in the visual cortex [13]. Furthermore, we have demonstrated that transplanted rod precursor cells, labeled by the rod-specific Nrl.GFP transgene, can significantly improve rod-mediated vision in the *Gnat1*$^{-/-}$ mouse model of night

blindness [13]. The degree of photoreceptor integration appears to be influenced by the host environment as different models of retinal degeneration allow varying levels of cell incorporation [15].

Human embryonic stem cells (ESC) and induced pluripotent cells (iPSC) currently represent the most feasible sources of cells for future cell therapies as they are renewable and can in principle give rise to all somatic cell types. While progress has been made in establishing *in vitro* differentiation protocols for photoreceptor cells, most have not yielded sufficient numbers or the appropriate stage for application in cell-based therapies [16-19]. Recently, in a landmark study, Sasai and colleagues described an embryoid body-based 3D ESC differentiation system, which recapitulated many aspects of normal retinal development, sparking the prospect of producing sufficient quantities of correctly-staged cells for clinical applications [20, 21]. Subsequently, we have shown that photoreceptor precursor cells isolated via expression of a Rho.GFP transgene from self-forming retinae (generated using an adapted Sasai protocol) have the ability to integrate into the healthy and degenerating retinal environment in mice [22]. These experiments demonstrated that a stem cell-based therapy for retinal dystrophies may in fact be possible by combining these new technologies.

One major obstacle preventing translation to the clinic is the lack of strategies to isolate and purify safe and effective cells from complex 3D tissue differentiation systems such as those generated from ESC or iPSCs. In these cultures the desired target cells are generated in addition to photoreceptors of inappropriate developmental stages and other undesired retinal and non-retinal proliferating and non-proliferating cell types. While transplantation-competent murine donor cells can be isolated relatively effectively from the developing retina via photoreceptor-specific

transgene expression [7, 12, 14, 15, 23] a similar genetic manipulation for clinical application is undesirable given the potential risks of tumorigenicity associated with genetic labelling techniques [24], as well as the need to overcome regulatory hurdles associated with combined cell- and gene-based therapies. The use of conjugated monoclonal antibodies specific to epitopes on the target cells constitutes an alternative to genetic tagging and has already been successfully deployed in clinical applications in the areas of cancer biology and immunology [25-27]. Previously, we identified two cell surface biomarkers, CD73 and CD24, that in combination labeled a (sub)population of postnatal photoreceptor precursor cells, and demonstrated that CD73/CD24 positive cells isolated from the postnatal mouse retina integrate efficiently into the normal and diseased mouse eye after sub-retinal transplantation [28]. CD73/CD24 double-positive rod precursors displayed a significantly higher integration potential than unsorted cells, or rod cells isolated using a conventional Nrl.GFP transgene. However, our data also indicated that additional markers would be necessary for isolation of photoreceptor precursor cells from heterogeneous stem cell differentiation cultures due to the broad distribution of individual cell surface antigens on non-photoreceptor cells [28]. Therefore, here we developed a cell surface biomarker panel of five markers that in combination permits the isolation of post-mitotic rod precursors from 3D ESC-derived self-forming retina. We show for the first time that ESC-derived rod precursors isolated via a photoreceptor precursor biomarker panel can integrate and mature into the normal or diseased adult mouse retina.

Material and Methods

Detailed methods are provided as Supplementary File 1

Results

Identification of cell surface biomarkers for photoreceptors

To identify a panel of useful cell surface antigens contributing to the characteristic biomarker signature of transplantation-competent photoreceptor precursors, defined as postnatal day 4-8 (P4-8) [13], we employed a dual approach. First, we examined microarray data of the P4 Nrl.GFP retina [28] for enrichment of genes encoding cluster of differentiation (CD) markers in the Nrl-expressing rod precursor population compared to other retinal cell types. CD markers represent cell surface molecules useful for cell immuno-phenotyping and already have widespread clinical application, (e.g. selection of bone marrow stem cells for transplantation [29]), due to the availability of well-established antibodies. Using a 2-fold cut off to delineate the positive and negative cell populations we identified 9 and 25 genes for known mouse CD markers that were enriched in rod precursors and other retinal cell types, respectively. An additional 60 CD marker genes were expressed in both populations in the P4 mouse retina (Supplementary Table 1).

In a second approach, we used flow-cytometry to screen postnatal retinal cells from Nrl.GFP mice with a panel of 174 well characterized monoclonal antibodies (BD Lyoplate screening panel) to CD markers and identified 15 expressed antigens (>2% in population; Supplementary Fig1A,B). A small number of markers labeled subsets of non-Nrl.GFP cells (e.g. CD309, CD200, CD15 and CD90), while the majority of cell surface antigens were common between retinal cell populations (Supplementary Fig1A,B). CD133 and CD73 intensely labeled Nrl.GFP cells compared to non-Nrl.GFP cells. Comparison of protein expression seen in the lyoplate screen to the respective mRNA levels of CD marker genes observed in the microarray analysis

(Supplementary Table 1) showed a widespread congruence, validating gene expression analysis as a useful means of identifying biomarkers for cell selection.

FACS analysis of the PPr biomarker panel during retinal development

We, and others, previously established that CD73 is photoreceptor-specific in the context of the developing retina, yet it also labels many other cell types, for example, mesenchymal stem cells [9, 28, 30]. Furthermore, CD73 is strongly expressed in late-stage and mature photoreceptors, which have poor transplantation efficiency and would therefore not be useful as a sole selection tool [12, 28]. To increase specificity, we examined CD73 co-labelling with additional CD markers. Based on their high expression levels in transplantation-competent Nrl.GFP rod precursors, we selected CD47 and CD133, together with CD73 and CD24, to test as a biomarker signature for positive cell selection (Supplementary Fig1A,B; in B, top right-hand quadrants of scatter plots show CD marker and Nrl.GFP co-labeled cells). All of the CD markers we identified on photoreceptor cells, are known to be expressed on other cell types, but no cell type has previously been defined as expressing this combination of CD markers [CD73(+)CD24(+)CD133(+)CD47(+)] together. To remove potentially harmful mitotically-active cells we utilised the retinal progenitor marker CD15 [31-33] for negative selection, which, as expected, did not show co-labeling of Nrl.GFP (Supplementary Fig1A, B). Henceforth, the combination of CD73(+), CD24(+), CD133(+), CD47(+) and CD15 (-) is referred to as the photoreceptor precursor (PPr) biomarker panel.

The PPr biomarker panel displayed a dynamic expression profile during the course of retinal histogenesis in flow cytometry analyses (Fig1A,B). At embryonic day 15 (E15) the proportion of cells expressing all four positive selection markers

(CD73, CD133, CD24 and CD47) was 3.5% ± 0.1 (Fig.1B; n=3), due to the low number of CD73 positive photoreceptors in the retina at this point. Over the next few days the proportion of CD73 positive cells increased resulting in an overall co-labelling of 17.9% ± 4.1 (Fig.1B; n=3) for the PPr marker panel at P4, which also represented the peak of co-expression of the biomarkers during retinal development. Among the CD73/CD133 double-positive cell population, which delineates the developing rods, CD24 and CD47, both markers of immature retinal cells, were also strongly expressed labelling 57.2% ± 17.5 and 96.3% ± 2.3 of the CD73/CD133 double positive population, respectively, at P4 (n=3; see Fig.1A for representative example). Subsequent developmental stages saw a reduction in the number of PPr panel-positive cells, with 10.9% ± 0.6 (Fig.1B; n=3) staining at P8 and only 6% ± 3.3 at P10 (Fig.1B; n=3). The decrease in co-labelling mainly occurred due to the down-regulation of CD24 in maturing retinal neurons. While CD47 expression was maintained at P10, it was then rapidly down-regulated and absent in mature photoreceptors (Supplementary Fig.2A). In a separate set of experiments, co-labelling for CD15 and CD73 showed that these two cell populations are mutually exclusive during retinal development indicating that CD15 can be used to remove progenitor cells from cell mixes (Fig.1C). qRT-PCR and immunohistochemical analysis was also performed on developing retinal samples and showed similar trends of biomarker expression (Supplementary Figure 2B, C). Taken together our data demonstrate that the PPr marker biomarker panel effectively labels developing, but not mature rod photoreceptors (Fig.1D).

Characterization of PPr biomarkers in 3D mESC differentiation cultures

Photoreceptor precursors can be generated efficiently using a previously described embryoid body-based 3D mouse ESC (mESC) differentiation system [20, 22]. In this culture system continuous neuroepithelia are readily produced within 5 days of differentiation and optic vesicle-like structures appear around day 7-9 (Fig.2 shows optic vesicle neuroepithelium at day 12). Retinal cell genesis proceeds in a sequence similar to normal retinal development with all neural retinal cell types being present and correctly organised in layers by day 29 of the differentiation procedure, a stage which has been shown to correlate with P4-8 during mouse retinal development [22].

Consistent with previous observations, we found that at day 12 of differentiation *in vitro* retinal epithelia showed widespread expression of retinal progenitor markers Pax6 and Vsx2 (Fig.2A,B), suggesting an immature state at this point. By day 27, the majority of cells within the retinal epithelium labeled with the rod markers Rhodopsin and Recoverin and displayed typical photoreceptor morphology (Fig.2C,D). Markers of advanced photoreceptor differentiation, such as rod α-Transducin and Peripherin 2, were only observed in a few photoreceptors at this point (Fig.2E, F). We assessed the expression profiles of PPr biomarker transcripts in this system using quantitative real-time PCR. Expression of all biomarkers could be detected in undifferentiated mESC cultures albeit at relatively low levels. During the retinal differentiation procedure, transcript levels of CD24, CD133, CD47 and CD15 increased from day 0 to day 12, while CD73 transcript levels were significantly increased by day 28; CD24 levels then declined by day 36 (Fig.2G). We also used an adeno-associated viral vector (pseudotype 2/9) carrying a GFP reporter under the control of a Rhodopsin promoter (Rhop.GFP) to label rod photoreceptors [22]. Importantly, real-time PCR on FAC-sorted Rhop.GFP-positive cells isolated at day 26 of culture confirmed

CD73, CD24, CD133 and CD47 expression in the rod population, whilst negligible levels of CD15 were detected (Fig.2H).

Next, we determined the spatial distribution of the proteins encoded by CD73, CD133, CD24 and CD47 using immunohistochemistry on tissue sections from early and late ESC differentiation cultures (Fig.2I-T). CD73 protein was not detected in early retinal epithelia at day 12 of differentiation but showed intense staining throughout the photoreceptor layer of *in vitro* retinae at day 28 and day 36, co-labelling with rod specific marker Rhodopsin and pan photoreceptor marker Recoverin. CD133, CD24 and CD47 showed a similar wide distribution across the retina during both early (day 12) and later (day 28) stages of differentiation, including the photoreceptor layer, and showed overlap with Rhodopsin and Recoverin signals. By day 36, CD24 co-labelling with Rhodopsin and Recoverin appeared reduced compared with earlier stages, and compared with the level of co-labelling observed for CD73, and CD133 (Fig 2K', N', Q'). In addition to the broad cell surface staining also observed with CD24 and CD47, CD133 displayed intense foci of immune-reactivity at the apical surface of the epithelium (Fig.2I; white arrowhead), similar to the pattern detected in late postnatal stages [28].

Taken together, these different components of the PPr biomarker panel are present at both transcript and protein levels in retinal differentiation cultures of mESC and exhibit an expression profile broadly consistent with that observed in the developing post-natal mouse retina.

FACS profile of PPr biomarkers during retinal differentiation in 3D cultures

We next established the percentage of cells labeled by each cell surface antigen at different times of the retinal differentiation protocol, by performing FACS analysis

using fluorochrome-conjugated antibodies (Fig.3A). In undifferentiated (day 0) mESC cultures CD73 weakly, but consistently, labeled a small number of cells. Labelling then increased significantly to 4.1% ± 2.7 at day 12, and 40% ± 7.9 at day 27 of differentiation consistent with onset of photoreceptor genesis in the *in vitro* retinae between the two later time points. In contrast, CD24 labeled most if not all cells at day 0 and displayed a slight decrease at subsequent stages of differentiation. CD133 and CD47 displayed a similar staining profile, labelling only a small proportion of cells at the start of the protocol (14.9% ± 8.2 and 18.1% ± 4.9 respectively) and increasing over time to 68.5% ± 21.4 and 81.8% ± 12.5 respectively, at day 27. These data suggest that no single marker would be sufficient to effectively isolate pure and stage-specific photoreceptor precursors for the purpose of retinal stem cell therapy.

We next investigated if, in combination, the cell surface biomarkers could be used to isolate cells displaying the typical photoreceptor precursor signature from the differentiation cultures at day 0, 12 and 27. As expected, at day 0 the number of cells expressing the PPr biomarker panel was minute (0.6% ± 0.1 at d0 and 1.2% ± 0.6 at d12, respectively). However, at day 27 of culture 24.6% ± 6.5 of all cells in the *in vitro* retinae were positive for the PPr marker combination (Fig.3B). Conversely, the retinal progenitor marker CD15 did not co-label with CD73 (Fig.3B), indicating that this marker would enhance removal of potential harmful cells prior to transplantation.

The distribution of CD markers is usually not restricted to one particular tissue or cell type. We therefore confirmed the identity of the PPr biomarker panel-positive cells generated in the 3D retinal culture system using immuno-cytochemistry (Fig.4A, B). Day 27 retina were dissociated and plated on coverslips to allow investigation of colocalisation of CD73 with Rhodopsin or Recoverin on a single cell basis.

Rhodopsin and Recoverin were selected as indicators of photoreceptor cell identity with robust available antibodies. We observed that 36.3%±14.4 (n=3) of the cells labeled with CD73. As expected, the majority of CD73 positive cells were also strongly co-labeled with the rod pigment rhodopsin (78.3% ± 10.5; n= 3), confirming the rod photoreceptor identity of PPr biomarker labeled cells generated in the day 27 ESC-derived retina. Similar analysis conducted using Recoverin showed co-labelling of 41% ± 13.6 (n=3) of the CD73 positive cells.

Of the total ESC-derived population, 45% ± 17.8 (n=3) showed Rhodopsin staining, confirming a robust and reproducible production of rod photoreceptors in this system. Approximately half of the total Rhodopsin-positive cells, expressed CD73 (49.4% ± 22.1) indicating the presence of photoreceptor precursors at different stages of development. Of the total ESC-derived population, 16.2% ± 7.1 (n=3) stained with Recoverin, with the majority of these Recoverin-expressing cells showing strong CD73 staining (92.9% ± 10.4; n=3).

We also performed immunostaining on cells plated after FACS selection using the PPr biomarker panel (CD+) compared with CD- and unsorted cells from day 27 ESC-derived cultures. Enrichment for Crx, Rhodopsin and Recoverin-positive cells was observed in the CD+ population (Figure 4C). Yields of PPr sorted CD+ cells ranged from 0.41 - 4.89 % of ESC cultures at day 27 (n=3) with a viability of 80%-90%. Together, these data indicate that the PPr biomarker panel is useful for the isolation of stage-specific rod photoreceptor cells from ESC-derived 3D retinal cultures.

Exclusion of mitotically active cells via PPr selection

Inclusion of undifferentiated pluripotent stem cells or other proliferating cell populations in cell preparations destined for transplantation presents a serious

challenge due to their propensity to result in uncontrolled growth and, in the worst case scenario, elicit the development of tumours [19, 34, 35]. It is essential that such cells be removed prior to transplantation to not only eliminate the risk of tumour formation but also increase integration efficiency of genuine photoreceptors as well as to prevent any permanent retinal detachment that could arise from cell masses in the sub-retinal space [13].

At day 27, a small number (<2%; n=3) of cells incorporated EdU during S-phase and 3.25% labeled with Ki67 (n=1) suggesting that this 3D retinal differentiation protocol is generally effective in promoting exit from cell cycle (Fig.5A). Nevertheless, because of inherent variability within culture preparations, further safeguards to stringently select against any persisting proliferative cells will be required. To test the ability of the PPr biomarker panel to remove mitotically active cells under challenging conditions (i.e. incomplete, less efficient differentiation) we added undifferentiated mouse embryonic stem cells (15%) to dissociated day 26 retinal cultures and determined the number of mitotic cells after FAC-sorting. No overlap was observed between EdU labelling and PPr biomarker selected cells (data not shown). However, we found that EdU labelling in combination with the five fluorochrome conjugated antibodies to the PPr biomarker panel was not very robust due to limitations in the detection system, therefore Ki67 antibody was used as an alternative quantitative labelling approach for mitotic cells. In these experiments, 21 ± 6.6% (n=3) of unsorted cells from the combined cell population (~15% undifferentiated ESC: 85% day 27 retinal cultures) showed Ki67 (+) staining (Fig.5B, C). Cells selected from this proliferative population via co-labelling with CD73+, CD24+, CD133+, CD47+, CD15- (CD+) contained only a very small number of Ki67(+) dividing cells (0.5% ± 0.23; n=3), demonstrating the effectiveness of the

biomarker panel even in the presence of contaminating, undifferentiated cells. On the other hand, a high proportion of proliferating cells were observed in the CD- population (46 ± 16.5; Fig.5B, C). These data demonstrate that mitotically-active cells are efficiently eliminated from donor cell populations, prior to transplantation, by using the combination of PPr cell surface biomarkers.

Transplantation of mESC derived photoreceptors

We next examined the transplantation potential of photoreceptors isolated via the PPr biomarker panel from mESC 3D retinal differentiation cultures. To this end, in a series of experiments, we transplanted 200,000 PPr biomarker FAC-sorted ESC-derived rod precursors into the subretinal space of adult wild type, and *Gnat1*$^{-/-}$ mice in which rods are non-functional due to the absence of the rod α–Transducin protein, pivotal to the phototransduction cascade [36]. ESC-derived rod precursors were sorted at day 27 of 3D retinal differentiation, based on their co-expression of the five specific PPr cell surface biomarkers CD73(+) CD24(+) CD133(+) CD47(+) CD15(-). Two methods were used in order to identify ESC-derived cells after transplantation. Either wEBs were infected with AAV2/9.CMV.GFP virus several days prior to the experiment, or, alternatively a transgenic mouse ESC line (CBA.YFP ESC; ATCC-R), with a YFP reporter cassette driven by the ubiquitously active beta-actin promoter was used.

Photoreceptors derived from both ESC lines, and selected via PPr biomarker expression (CD+) integrated into the adult mouse retina after subretinal injection (Fig.6A-E; Supplementary Fig.3). Three weeks post transplantation GFP/YFP labeled cells, with single nuclei and displaying the characteristic rod morphology, were readily visible within the outer nuclear layer (ONL) of recipient mice and were

frequently found in small clusters near the injection site (Fig.6). Rod α–Transducin (Gnat-1) immunostaining was detected in the outer segments of GFP-labeled cells integrated into ONL of wild type and in the Gnat-deficient recipient retina (Fig.6A, C; Supplementary Fig.3). In the latter, we observed clear and robust expression of the outer segment protein (Gnat-1) that was missing in the endogenous rods in the knock out model. The YFP/GFP-labeled cells displayed typical rod features such as segment formation and spherical synaptic connections in the outer plexiform layer. Furthermore, integrated cells were Recoverin (Fig.6B) and Rhodopsin positive but did not stain with cone-specific markers such as RxRγ, sw-opsin and mw-opsin (data not shown) demonstrating a rod identity of incorporated cells. Transplantations of cells selected via PPr biomarker expression (CD+) from the mouse postnatal day 8 (P8) Nrl.GFP retina similarly showed integration of GFP+ cells within the recipient wild type ONL three weeks later (Supplementary Figure 3). We evaluated the efficiency of transplantation using the PPr biomarker selected ESC-derived photoreceptor precursors by counting the number of new GFP-labeled cells integrated within the recipient ONL. The transgenic mouse ESC line (CBA.YFP), rather than viral labelling, was used for quantification experiments as contaminating viral particles could hypothetically label host photoreceptors [22]. Indeed, in experiments using AAV2/9.CMV.GFP virus, we observed a large number of integrated GFP-labeled cells did not co-label with Gnat-1, suggesting that either some integrated cells had not yet acquired a mature differentiation state, which can take many days [14], or that a proportion of GFP+ cells were a product of viral labelling of host cells (data not shown).

We found that transplantation of the PPr biomarker positive CBA.YFP ESC-derived photoreceptor precursors resulted in integration levels significantly higher

than unsorted cells (Fig.6G; median for CD**+** = 654 cells, range of total number of integrated cells per retina = 315 - 1068, N=7), and similar to those previously reported with virally-labeled Rhop.GFP ESC-derived rods [22]. By contrast, transplantation of biomarker negative cells (CD**-**), or unsorted day 27 ESC cultures demonstrated only poor integration abilities (Fig.6F; median for CD**-** = 9 cells, range 0 - 204, N=6; median for unsorted day 27 cultures cells = 60, range 0 - 80, N=6). We observed integration levels for P8 PPr biomarker positive cells similar to those for ESC-derived PPr biomarker positive cells (median = 210 cells, range 22 - 3039 N=9). In all ESC transplants, non-integrated GFP+ ESC-derived cells typically persisted in the subretinal space 3 weeks after injection (Supplementary Fig.3C shows cells in subretinal space in low magnification view of Fig.6E). In transplants of biomarker negative cells (CD**-**) we frequently observed large sub-retinal cell masses that contained unidentified cell types of diverse morphologies (Fig.6F) but little or no integration. Immmunostaining for Pax6 and GFAP, markers of immature neurons and glial cells respectively, and Ki67 for mitotically active cells, did not label significant numbers of cells in the PPr biomarker panel negative sub-retinal cell masses at 3 weeks post transplantation (data not shown). Taken together, these data demonstrate that FAC-sorted ESC-derived rod precursors selected via the PPr biomarker panel from dissociated synthetic retinae can integrate effectively, and significantly more efficiently than the unsorted ESC-derived cells or PPr biomarker negative populations.

Conservation of biomarkers in the developing and mature human retina

To test the usefulness of the biomarker panel for clinical application we investigated the expression of CD73, CD133, CD24 and CD47 in the human retina. RT-PCR

revealed CD24 and CD47 were abundantly expressed even at the early stages of retinal development (8wks gestation) and, in contrast to the murine retina, remained at similar levels in the mature tissue (Fig.7A). CD133 was expressed at low levels during weeks 9, 10 and 11 but increased thereafter and was strongly expressed at the adult stage. In contrast, CD73 mRNA was not detected until 12wk of gestation and was present at all subsequent stages of development and in the mature retina.

In order to establish the spatial distribution of the biomarker proteins we performed immunohistochemistry on cryo-sections prepared from human fetal and adult retinal tissue. At 10, 13 and 19wk of gestation, CD24 and CD47 proteins were detected in all retinal layers (Fig.7B; Supplementary Fig.4) including the developing outer nuclear layer, which contained CRX and RECOVERIN positive photoreceptor precursor cells. While CD73 transcript was present from 12wk onwards, no immunostaining was observed during the fetal stages, suggesting a post-transcriptional control mechanism. In contrast, CD133 protein was visible starting from 10wks in a punctate pattern at the apical surface of the retina, abutting the interface with the retinal pigmented epithelium. qRT-PCR analysis of expression of the PPr biomarker panel genes in human retinal samples showed expression of CD47 and CD24 during fetal stages, but decreased expression in the mature retina (Supplementary Figure 4B), in line with the reduced labelling of mature photoreceptors by these markers in the human and mouse retina (Supplementary Figure 4A, Supplementary Figure 2).

While CD73 protein appeared to be absent in the native fetal human retina, a small number of CD73 immuno-positive cells were observed in differentiation cultures derived from 14wk old primary retinal cells (Fig.7C). Approximately 6% of cells in these primary cultures co-labeled with CD73 and CD133 in FACS analysis,

whereas 39.4 ± 4.76% of cells in the adult human retina were positive for this dual marker combination (Fig.7D). The total number of cells in the adult retina labelling with CD73 was 74 ± 4.7%, consistent with the total number of photoreceptors (Fig.7D). Furthermore, in immunocytochemical analysis of dissociated retinal cells all CD73 positive cells in the adult human retina co-expressed Recoverin, indicating a photoreceptor identity (Fig.7E).

Taken together, our findings demonstrate that the expression patterns and relative onset of biomarker expression with respect to retinal differentiation is similar between mouse and human. The lack of available human fetal tissue beyond 19wk of gestation prevented us from pinpointing the exact onset of CD73 protein expression in the human retina; most rod photoreceptors are generated after 19 wks. However, our observations are consistent with findings in the murine retina, which showed onset of CD73 protein expression in the postnatal time period when the majority of the rod photoreceptors are born and then sustained expression in photoreceptors.

Discussion

Cell replacement therapy for retinal disease is a very promising therapeutic strategy currently under investigation, the goal of which is the transplantation of stem cell-derived cells into the diseased retina, either to substitute photoreceptor cells lost through the disease process and replace disease genes, or to delay or prevent the loss of the remaining cells [37, 38]. We and others have demonstrated that photoreceptor precursors can be introduced into the normal and degenerating rodent retina via sub-retinal injection and that transplanted rods make appropriate synaptic connections to the remaining inner retinal cells [7-10, 15]. Furthermore, correctly

integrated cells have been shown to confer low light visual function in a mouse model of retinal degeneration and signals generated by these cells were projected to visual processing areas in the brain [13].

The most promising sources of donor cells for a future therapeutic application are hESCs and iPSCs; however, the successful translation of this approach to the clinic is critically dependent on the development of methods for the isolation and purification of optimal stage precursor cells. The use of mixed cell populations carries the risk of tumorigenesis due to the presence of mitotically active stem cells, and even inappropriately staged photoreceptors reduce integration efficiency and therefore would result in a suboptimal clinical outcome. It is therefore critical that a cell selection strategy should enable the specific isolation of wild type cells, which are committed to the photoreceptor lineage, but which have not yet fully matured, as well as excluding proliferating cells.

In order to meet the need for stringent cell selection and avoiding genetic manipulation of cells, we have developed a panel of five useful photoreceptor biomarkers that can be effectively utilised to isolate transplantation-competent rod precursors from 3D retinal differentiation cultures of mESC. In this study we utilised existing CD markers for which fluorochrome-conjugated antibodies already exist far application in FACS protocols. Although we have not formally proved that all five selected CD markers are necessary and sufficient, this study demonstrates for the first time the successful application of a CD marker signature for isolation of photoreceptor precursors from differentiated ESCs. In future work it may be possible to develop antibodies suitable for FACs for additional markers identified in photoreceptors by microarray analysis [28, 39]. We selected CD73 and CD133 to confer photoreceptor specificity in the context of ESC-derived retinal differentiation

cultures and CD24 and CD47 to enrich for cells equivalent to young, postnatal cells. In addition CD15 (SSEA-1) was included for negative cell selection. We showed that the biomarkers for positive cell selection (CD73, CD133, CD24 and CD47) have a peak of co-expression that correlates with the window of transplantation competence (P4-P8) for donor cells isolated from the developing retina. Importantly, the expression of individual biomarkers in mESC differentiation cultures followed the same pattern seen in the developing retina, with 25% of cells in day 27 cultures displaying the biomarker signature of transplantation-competent rod precursors. The majority of CD73-expressing cells (~85%) in day 27 cultures co-labeled with the rod marker Rhodopsin. Our data indicate that the PPr biomarker selection panel strongly enriches for immature photoreceptors in the context of this very heterogeneous ESC-derived retinal cell culture system.

Consistent with this conclusion, we showed that sub-retinal transplantation of cells selected via the PPr biomarker panel (CD+) resulted in significantly higher integration levels compared to unsorted cells, or cells that did not label with the positive-selection markers (CD-). While integrated CD+ cells displayed the typical rod morphology and labeled with Recoverin, CD- cells rarely integrated and instead formed substantial cell masses with varying morphology. These observations illustrate heterogeneity present in the ESC retinal culture system and the effects of inclusion of non-photoreceptor cells in cell preparations. Significantly, we showed that the PPr biomarker panel selection excludes proliferating cells, as assessed by Ki67 labelling, even in samples comprising more than 10% mitotically active stem cells.

This study brings together for the first time the use of photoreceptor cell sorting strategies using CD markers, and new ESC-derived self-forming retinal cultures to

isolate transplantation-competent cells without genetic modification. This is an important milestone towards the development of clinical photoreceptor cell therapy. The biomarker-sorted cells maintained viability and showed integration levels similar to those observed using genetically-labeled ESC-derived populations [22]. As the integration levels achieved with the ESC-derived cells and the PPr biomarker selection panel were lower than previously reported experiments using CD73/CD24 selected cells (Median 10,899, range 544-32,826, [28]; Mean 2199 ± 1006 cells/retina [9],) and Nrl.GFP selected cells (Mean 16,759 ± 1,705 cells/retina [13]), isolated from the developing retina, further optimization and fine tuning of differentiation and isolation protocols will be required to maximize the transplantation outcome. Variability in transplant outcomes as reflected in the range of integrated cell numbers, possibly due to variation in host inflammatory responses and surgical delivery of cells [14, 40, 41] also needs to be resolved in future studies. Based on our previous demonstration of restoration of visual function in the *Gnat1*$^{-/-}$ model containing ~25,000 newly-integrated cells from the developing retina [13], we estimate that a 40-fold increase in the number of integrating ESC-derived cells will be required to demonstrate robust restoration of rod function in a mouse model *in vivo.*

Lastly, the fact that the expression of components of the photoreceptor biomarker panel was conserved in the developing and adult human retina suggests that our cell selection approach may be applicable for isolation of cells for clinical transplantation from human ESC/iPSC retinal culture systems. Taken together, we have identified and tested, for the first time, a set of 5 cell surface biomarkers that are useful for the enrichment of transplantation-competent rod photoreceptor cells from pluripotent stem cell-derived self-forming retina. These findings define an

approach that we anticipate will be broadly applicable for the isolation of photoreceptor cells for clinical therapy.

Figure legends

Figure 1. Expression of the photoreceptor biomarker panel during retinal development in the mouse. (A) Representative FACS scatter plots showing co-immunostaining of individual cell surface markers at different time point during retinal histogenesis. Dependent gates are shown from left to right. (B) Summary of FACS analysis for combined photoreceptor biomarker panel and CD73 alone. While CD73 alone efficiently labels all post mitotic photoreceptor cells, including non-integration competent adult photoreceptors, the biomarker panel enriches for cells from a narrow postnatal time window, which coincides with transplantation competence. (C) Assessment of co-expression of retinal progenitor marker CD15 and CD73 at postnatal day 4. CD15 and CD73 are mutually exclusive during retinal development. (D) Schematic showing a comparison of the relative onset of expression of key photoreceptor markers and individual cell surface biomarkers. Vertical bars denote the optimal transplantation competent period for photoreceptor precursors (P4-P8).

Figure 2. Characterization of PPr surface biomarkers on 3D ESC retinal cultures.

(A, B) Day 12 optic vesicle neuroepithelium showing Vsx2 (green, A) and Pax6 (red, B) positive retinal progenitor cells. (C, D) Day 28 retinal neuroepithelium regions containing Rhodopsin (green, C) and Recoverin (red, D) positive ESC-derived photoreceptors. (E, F) Immunohistochemical analysis showing a small number of cells positive for Rod α-transducin (E) and Peripherin 2 (F) at day 28 of culture. High magnification inserts highlight expression pattern of these markers. (G) Real time quantitative RT-PCR analysis of ESC retinal cultures demonstrating the expression of PPr biomarker panel over time in culture. (H) Expression of the PPr biomarker

panel on day 26 FAC-sorted Rhop.GFP+ ESC-derived rods. (I) Immunohistochemical analysis for CD73, CD24, CD133 and CD47 (red), and Recoverin and Rhodopsin (green) on cryosections of ESC-retinal differentiations at day 12, 28 and 36 of culture. Scale bars: 25μm

Figure 3. Expression of components of the photoreceptor biomarker panel during mESC differentiation. (A) Representative fluorescent activated cell sorting (FACS) scatter plots showing the expression of individual cell surface markers in undifferentiated mESC and at day 12 as well as day 27 of the retinal differentiation procedure. A summary of three experiments is shown to the right of the plots. (B) FACS analysis of PPr biomarker panel at day 12, 27 and 36 of mESC differentiation. At day 27 (scatter plots shown) about 25% of the cells in the differentiating embryoid bodies express the combination of cell surface markers characteristic for postnatal photoreceptors but do not co-label with progenitor marker CD15. By day 36 < 1% of total cell population expresses the PPr biomarker panel. FSC, forward scatter.

Figure 4. Majority of CD73 positive cells in ESC-derived retinal cultures express photoreceptor markers. (A) Immunocytochemical analysis of cells from dissociated ESC retinal cultures co-stained with cell surface biomarker CD73 and photoreceptor markers Rhodopsin or Recoverin. Representative confocal tile scan of plated cells. Inset show high magnification view of indicated area. (B) Image analysis software Cellprofiler was used to determine the number of single or double positive cells from three independent experiments and confirmed by manual counting. Total number of marker positive cells is shown as light bars while darkly shaded bars indicate the percentage of cells co-staining for the respective second marker. About 44% of all cells express rhodopsin, 29% CD73 and 16% show Recoverin staining. The majority

of CD73 positive cells (~82%) label with rod photoreceptor marker rhodopsin and ~40% label with Recoverin. (C) Analysis of cells selected from ESC-derived day 27 retinal cultures using PPr biomarker panel (CD+). Immunocytochemical analysis of CD+ selected cells, CD- and unsorted ESC-derived cells with photoreceptor markers CRX, Rhodopsin or Recoverin was used to determine the number of cells expressing each marker (n= 3 independent experiments). 82.64 ± 7.53%, 76.83 ± 9.6%, and 17.3 ± 4.9% of CD+ cells labelled with photoreceptor markers CRX, Rho, and REC respectively; Mean ± SD. Scale bars: 40 μm

Figure 5. FAC-sorting via PPr biomarker panel eliminates mitotically active cells. (A) Representative FACS scatter plot of EdU based proliferation assay, following a 2 hour EdU pulse, showing percentage of d26 ESC retinal culture cells in S-phase of cell cycle. Only 2% of cells have incorporated EdU demonstrating that the majority of ESC-derived cells are postmitotic. (B) Undifferentiated mESC (15%) were added to dissociated d26 retinal cultures and the resulting cell suspension was sorted via PPr biomarkers. CD(+), CD(-) and unsorted cells were plated for immunocytochemical analysis and the number of Ki67+ cells was determined using Cellprofiler software. (C) Summary of Ki67 based proliferation assay. FACS sorting using PPr biomarkers effectively removed Ki67+, mitotically active cells from the cell sample. FSC, forward scatter. DAPI, blue, Ki67, red. Scale bars: 200 μm

Figure 6. Transplantation of mESC-derived, biomarker sorted photoreceptor precursors into the adult mouse retina. (A) Virally-labeled day 27 ESC-derived photoreceptor precursors sorted via biomarker panel integrated into *Gnat1*$^{-/-}$ adult retina. Anti-Gnat-1 immunohistochemistry only labels the outer segments of transplanted cells but not host photoreceptors. (B) Whole embryoid bodies from the

CBA.YFP mESC line endogenously expressing YFP; day 27 of retinal differentiation cultures were FAC-sorted via PPr biomarker panel and transplanted sub-retinally into adult wild-type retinas (B, C, D, E, F). (C, D) Cells expressing the biomarker panel (CD+) integrate into the outer nuclear layer (ONL) of the host, while cells from the biomarker negative fraction (CD-) did not integrate and formed large cell clusters in the subretinal space. (E) Summary of data from subretinal transplantation experiments showing numbers of cell integrates within the outer nuclear layer 3 weeks post transplantation. (F) Transplanted cells, which have migrated into the ONL express photoreceptor marker Recoverin. Inset show a high magnification view of the area indicated by arrow. Scale bars, 20 μm.

Figure 7. Expression of PPr biomarker panel components in the human retina. (A) RT-PCR analysis showing the expression of biomarkers at different stages of development in the human retina. CD24 and CD47 transcripts are strongly expressed prior to the F1 stage, while CD133 shows only weak levels of expression and CD73 is absent. CD73 transcripts are first observed at 11 weeks of gestation correlating with the onset of photoreceptor development. (B) Immunohistochemistry analysis of cell surface and key retinal markers at 19wk of gestation. CD24 and CD47 display a widespread expression pattern, labelling cells in all retinal layers. CD133 immunostaining is restricted to punctate labelling at the apical surface of the developing outer nuclear layer, whereas CD73 staining is absent at this stage. White arrows indicate region of higher magnification inset for CD133 and CD73. (C) Immunocytochemical analysis of 14 wk cultured fetal human cells. Cells expressing CD133, CD47 and CD24 are abundant at the beginning of culture, CD73 positive cells only begin to appear after two weeks in culture. (D) FACS analysis of cultured fetal cells at 14wk and adult human retinas. A small number of CD73/CD133 double

positive cells are present in primary cell cultures derived from 14wk retinas. In the adult human retina ~78% of cells express CD73 and ~40% co-label with CD133, consistent with the murine retina. (E) Colabelling immunocytochemistry of dissociated adult retinal cells showing all CD73+ cells express the photoreceptor marker recoverin. ONL, outer nuclear layer; ONBL, outer neuroblastic layer; INL, inner nuclear layer; GCL, ganglion cell layer. Scale bars: 20 μm

Supplementary Material

Supplementary Table 1. CD surface marker analysis from P4 Nrl.GFP microarray. Genes encoding for cluster of differentiation (CD) markers expressed in the postnatal day 4 mouse retina. Genes are grouped according to their enrichment in the rod precursor population (Nrl.GFP+), other retinal cell types (Nrl.GFP-), or ubiquitous expression. The log intensity indicates relative signal strength in the microarray experiment and fold change is given as a measure of enrichment between positive and negative cell populations. A fold change value of 2 was used to delineate the two cell populations. Markers used in PPr biomarker panel are highlighted in green.

Supplementary Figure 1. Cell surface marker screen of P8 Nrl.GFP retinae using BD Lyoplates. (A) Heat map showing top 15 cell surface marker candidates identified in the FACS-based screen. The relative number of cells in the Nrl.GFP positive and Nrl.GFP negative cell populations is indicated (red, high; green, low). (B) Individual flow cytometry scatter plots of dissociated P8 retinal cells for cell surface markers identified in the lyoplate screen. Nrl.GFP intensity is plotted on the x-axis whereas

staining intensity of the cell surface markers is shown on the individual y-axes. Top right hand quadrants of scatter plots show CD marker and Nrl.GFP co-labeled cells

Supplementary Figure 2. A, Flow cytometry analysis of cell surface marker CD47 during postnatal retinal development. At postnatal day 4 and 8, CD47 is expressed in most, if not all, retinal cells but is down-regulated in more mature Nrl.GFP expressing rod photoreceptors at day 21. B, Real time quantitative RT-PCR analysis of mouse retina demonstrating the expression of PPr biomarker panel over time. C, Immunohistochemical analysis for CD73, CD133, CD24, CD47, CD15, (red), on cryosections of P1, P7 and adult Nrl.GFP (green) retina. CD73 and CD133 co-localize in developing and mature photoreceptors, whereas initially broad expression of CD24 and CD47 is down-regulated in adult photoreceptors. CD15 is seen only in amacrine processes within the inner plexiform layer at these timepoints. NBL, neuroblastic layer; IPL, inner plexiform layer; GCL, ganglion cell layer; ONL, outer nuclear layer; INL, inner nuclear layer. Scale bars: 20μm.

Supplementary Figure 3. A'-A''', Transplants of PPr biomarker panel selected cells from P8 mouse retina (Nrl.GFP) into wild type recipients. 3 weeks after subretinal injection, PPr selected GFP-positive photoreceptors were observed within the recipient ONL. B-D Immunohistochemical analysis of integrated rod photoreceptors derived from a YFP expressing mouse embryonic stem cell line and CD biomarker selected (CD+), 3 weeks after sub-retinal transplantation in wild-type mice. B-C, Z-stack maximum projection showing integrated YFP-expressing photoreceptors co-labelling with the rod specific phototransduction protein GNAT-1 in the host outer nuclear layer. Dashed square indicates the location of the high magnification image of a single slice of Z-stack. D, Low magnification view of CD+ transplanted cells

surviving in the subretinal space, corresponding to region shown in Figure 6E. White arrows in D' indicate the location of the inset high magnification image; location of asterisks in the inset plate correspond to the location of the arrows. IS, inner segment; OPL, outer plexiform layer; ONL, outer nuclear layer; INL, inner nuclear layer; Scale bars: 20μm

Supplementary Figure 4. A**,** Immunohistochemical expression analysis of biomarkers in the developing and adult human retina. At 10, 13 and 19 weeks of gestation, CD24 and CD47 are expressed broadly across all retinal layers while CD133 is restricted to bright foci on the apical side of the outer neuroblastic layer abutting the retinal pigment layer. Immunostaining for CD73 on the other hand is not visible at these stages. At 19 weeks, CD24 and CD47 staining is particularly strong in the emerging inner plexiform layer, developing interneurons in the inner nuclear layer as well as nerve fibre layer. In the adult retina, CD73 expression can be observed in the ONL and CD133 is localized to the base of outer segments of photoreceptors. Both CD24 and CD47 are down regulated in the adult photoreceptor layer, while strong CD47 immuno-labelling is visible in the INL and OPL. By 10wks CD15 is down regulated in neuroblasts, and is detected transiently in projections of presumed amacrine cells in the IPL at 19wks. B, Real time quantitative RT-PCR analysis of the expression of the PPr biomarker panel over time in human retinal samples. CD24 and CD47 are downregulated in the adult retina compared with the fetal retina; expression patterns of the biomarkers during human and mouse retinal development are largely consistent (see Supplementary Figure 2). ONBL, outer neuroblastic layer; GCL, ganglion cell layer; INBL, inner neuroblastic layer; ONL , outer nuclear layer; INL, inner nuclear layer; IS, inner segments; OS, outer segments; IPL, inner plexiform layer. Scale bars 20μm

Acknowledgments

We thank the UCL Institute of Child Health flow cytometry facility (A. Eddaoudi, A. Rose, T. Adejumo) for FACS assistance, and the confocal facility (Bertrand Vernay) for technical support. This work was supported by the Medical Research Council UK (G0901550 and mr/j004553/1); Fight for Sight; Child Health Research Appeal Trust; NIHR Biomedical Research Centre for Pediatric Research at Great Ormond Street Hospital for Children and UCL Institute of Child Health; National Institute for Health Research (NIHR) Biomedical Research Centre for Ophthalmology at Moorfields Eye Hospital and UCL Institute of Ophthalmology; the human embryonic and fetal material was provided by the Joint Medical Research Council UK (grant# G0700089)/Wellcome Trust (grant # GR082557) Human Developmental Biology Resource (http://hdbr.org). R.A.P. is a Royal Society University Research Fellow and J.C.S. is funded by the Great Ormond Street Hospital Children's Charity. JWBB is a NIHR Research Professor.

Potential Conflicts of Interest

None

Reference List

1. Sohocki MM, Daiger SP, Bowne SJ et al. Prevalence of mutations causing retinitis pigmentosa and other inherited retinopathies. **Hum Mutat**. 2001;17:42-51.
2. Hartong DT, Berson EL, Dryja TP. Retinitis pigmentosa. **Lancet**. 2006;368:1795-1809.
3. Punzo C, Kornacker K, Cepko CL. Stimulation of the insulin/mTOR pathway delays cone death in a mouse model of retinitis pigmentosa. **Nat Neurosci**. 2009;12:44-52.
4. Resnikoff S, Keys TU. Future trends in global blindness. **Indian J Ophthalmol**. 2012;60:387-395.
5. Resnikoff S, Pascolini D, Etya'ale D et al. Global data on visual impairment in the year 2002. **Bull World Health Organ**. 2004;82:844-851.
6. Koberlein J, Beifus K, Schaffert C et al. The economic burden of visual impairment and blindness: a systematic review. **BMJ Open**. 2013;3:e003471.
7. Bartsch U, Oriyakhel W, Kenna PF et al. Retinal cells integrate into the outer nuclear layer and differentiate into mature photoreceptors after subretinal transplantation into adult mice. **Exp Eye Res**. 2008;86:691-700.
8. Eberle D, Kurth T, Santos-Ferreira T et al. Outer segment formation of transplanted photoreceptor precursor cells. **PLoS One**. 2012;7:e46305.

9. Eberle D, Schubert S, Postel K et al. Increased integration of transplanted CD73-positive photoreceptor precursors into adult mouse retina. **Invest Ophthalmol Vis Sci**. 2011;52:6462-6471.

10. Lamba DA, Gust J, Reh TA. Transplantation of human embryonic stem cell-derived photoreceptors restores some visual function in Crx-deficient mice. **Cell Stem Cell**. 2009;4:73-79.

11. Lamba DA, McUsic A, Hirata RK et al. Generation, purification and transplantation of photoreceptors derived from human induced pluripotent stem cells. **PLoS One**. 2010;5:e8763.

12. MacLaren RE, Pearson RA, MacNeil A et al. Retinal repair by transplantation of photoreceptor precursors. **Nature**. 2006;444:203-207.

13. Pearson RA, Barber AC, Rizzi M et al. Restoration of vision after transplantation of photoreceptors. **Nature**. 2012;485:99-103.

14. Warre-Cornish K, Barber AC, Sowden JC et al. Migration, integration and maturation of photoreceptor precursors following transplantation in the mouse retina. **Stem Cells Dev**. 2014;23:941-954.

15. Barber AC, Hippert C, Duran Y et al. Repair of the degenerate retina by photoreceptor transplantation. **Proc Natl Acad Sci U S A**. 2013;110:354-359.

16. Lamba DA, Karl MO, Ware CB et al. Efficient generation of retinal progenitor cells from human embryonic stem cells. **Proc Natl Acad Sci U S A**. 2006;103:12769-12774.

17. Meyer JS, Shearer RL, Capowski EE et al. Modeling early retinal development with human embryonic and induced pluripotent stem cells. **Proc Natl Acad Sci U S A**. 2009;106:16698-16703.

18. Osakada F, Ikeda H, Mandai M et al. Toward the generation of rod and cone photoreceptors from mouse, monkey and human embryonic stem cells. **Nat Biotechnol**. 2008;26:215-224.

19. West EL, Gonzalez-Cordero A, Hippert C et al. Defining the integration capacity of embryonic stem cell-derived photoreceptor precursors. **Stem Cells**. 2012;30:1424-1435.

20. Eiraku M, Takata N, Ishibashi H et al. Self-organizing optic-cup morphogenesis in three-dimensional culture. **Nature**. 2011;472:51-56.

21. Nakano T, Ando S, Takata N et al. Self-formation of optic cups and storable stratified neural retina from human ESCs. **Cell Stem Cell**. 2012;10:771-785.

22. Gonzalez-Cordero A, West EL, Pearson RA et al. Photoreceptor precursors derived from three-dimensional embryonic stem cell cultures integrate and mature within adult degenerate retina. **Nat Biotechnol**. 2013;31:741-747.

23. Lakowski J, Baron M, Bainbridge J et al. Cone and rod photoreceptor transplantation in models of the childhood retinopathy Leber congenital amaurosis using flow-sorted Crx-positive donor cells. **Hum Mol Genet**. 2010;19:4545-4559.

24. Mukherjee S, Thrasher AJ. Gene therapy for PIDs: progress, pitfalls and prospects. **Gene**. 2013;525:174-181.

25. Huang PY, Best OG, Belov L et al. Surface profiles for subclassification of chronic lymphocytic leukemia. **Leuk Lymphoma**. 2012;53:1046-1056.

26. Yang YM, Chang JW. Current status and issues in cancer stem cell study. **Cancer Invest**. 2008;26:741-755.

27. Woodward WA, Sulman EP. Cancer stem cells: markers or biomarkers? **Cancer Metastasis Rev**. 2008;27:459-470.

28. Lakowski J, Han YT, Pearson RA et al. Effective transplantation of photoreceptor precursor cells selected via cell surface antigen expression. **Stem Cells**. 2011;29:1391-1404.

29. Gaspar HB, Parsley KL, Howe S et al. Gene therapy of X-linked severe combined immunodeficiency by use of a pseudotyped gammaretroviral vector. **Lancet**. 2004;364:2181-2187.

30. Iser IC, Bracco PA, Goncalves CE et al. Mesenchymal Stem Cells From Different Murine Tissues Have Differential Capacity to Metabolize Extracellular Nucleotides. **J Cell Biochem**. 2014.

31. Koso H, Iida A, Tabata Y et al. CD138/syndecan-1 and SSEA-1 mark distinct populations of developing ciliary epithelium that are regulated differentially by Wnt signal. **Stem Cells**. 2008;26:3162-3171.

32. Koso H, Ouchi Y, Tabata Y et al. SSEA-1 marks regionally restricted immature subpopulations of embryonic retinal progenitor cells that are regulated by the Wnt signaling pathway. **Dev Biol**. 2006;292:265-276.

33. Klassen H, Ziaeian B, Kirov, II et al. Isolation of retinal progenitor cells from post-mortem human tissue and comparison with autologous brain progenitors. **J Neurosci Res**. 2004;77:334-343.

34. Arnhold S, Klein H, Semkova I et al. Neurally selected embryonic stem cells induce tumor formation after long-term survival following engraftment into the subretinal space. **Invest Ophthalmol Vis Sci**. 2004;45:4251-4255.

35. Chaudhry GR, Fecek C, Lai MM et al. Fate of embryonic stem cell derivatives implanted into the vitreous of a slow retinal degenerative mouse model. **Stem Cells Dev**. 2009;18:247-258.

36. Calvert PD, Krasnoperova NV, Lyubarsky AL et al. Phototransduction in transgenic mice after targeted deletion of the rod transducin alpha -subunit. **Proc Natl Acad Sci U S A**. 2000;97:13913-13918.

37. Lamba D, Karl M, Reh T. Neural regeneration and cell replacement: a view from the eye. **Cell Stem Cell**. 2008;2:538-549.

38. West EL, Pearson RA, MacLaren RE et al. Cell transplantation strategies for retinal repair. **Prog Brain Res**. 2009;175:3-21.

39. Postel K, Bellmann J, Splith V et al. Analysis of cell surface markers specific for transplantable rod photoreceptors. **Mol Vis**. 2013;19:2058-2067.

40. West EL, Pearson RA, Barker SE et al. Long-term survival of photoreceptors transplanted into the adult murine neural retina requires immune modulation. **Stem Cells**. 2010;28:1997-2007.

41. Pearson RA, Hippert C, Graca AB et al. Photoreceptor replacement therapy: challenges presented by the diseased recipient retinal environment. **Vis Neurosci**. 2014;31:333-344.

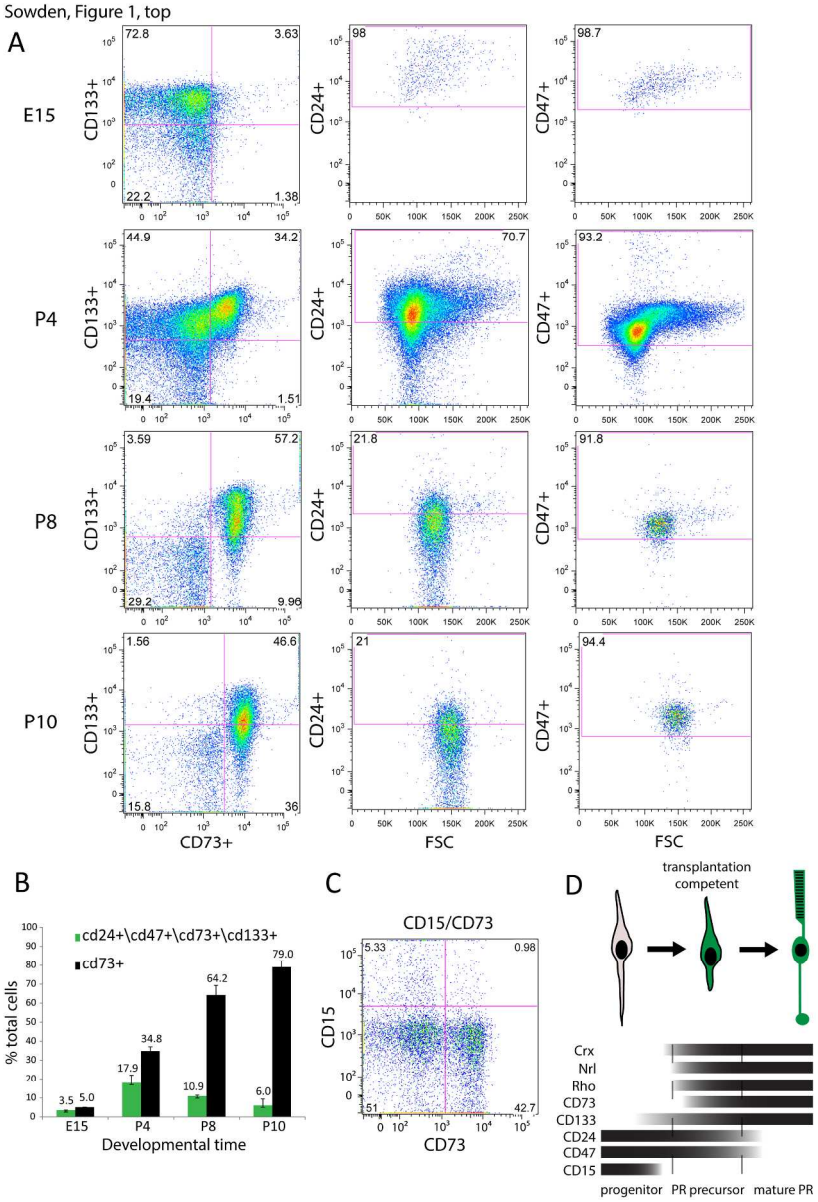

Figure 1
187x274mm (300 x 300 DPI)

Sowden, Figure 2, top

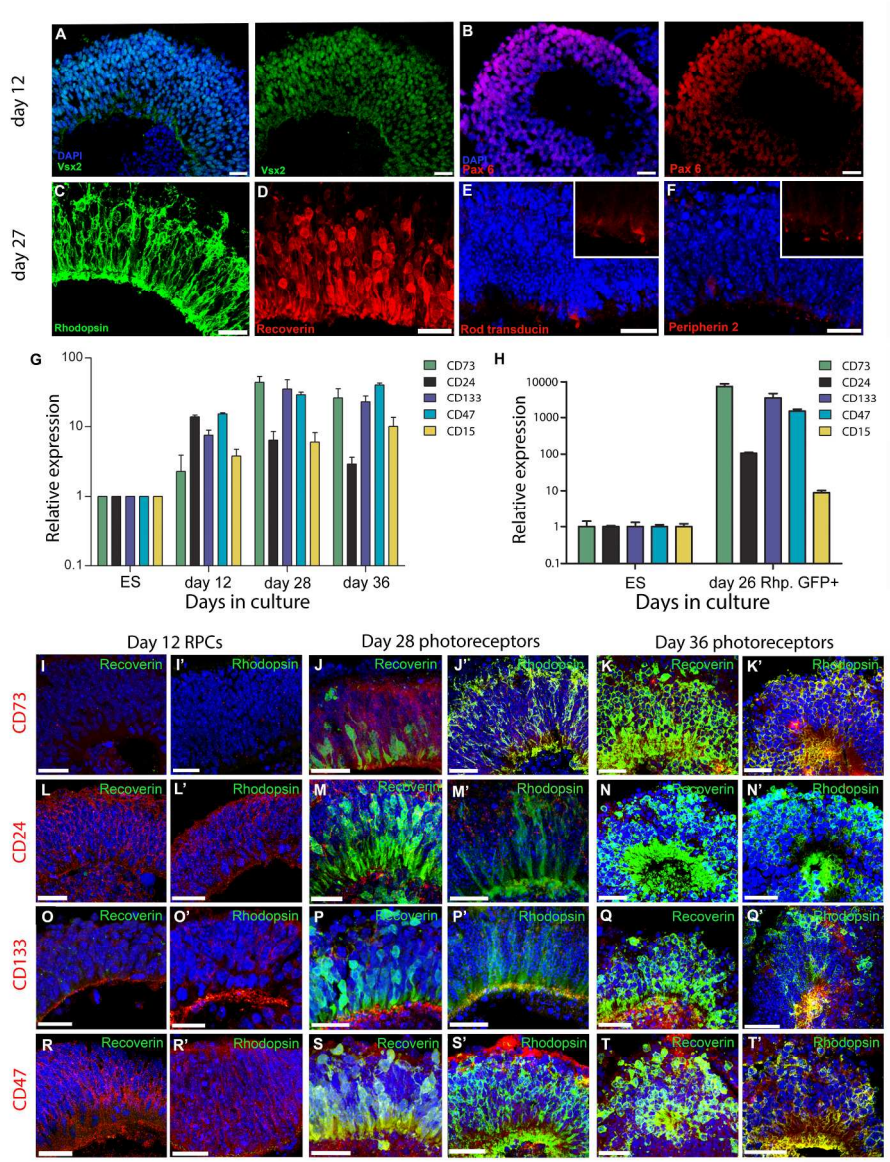

Figure 2 R1
203x270mm (300 x 300 DPI)

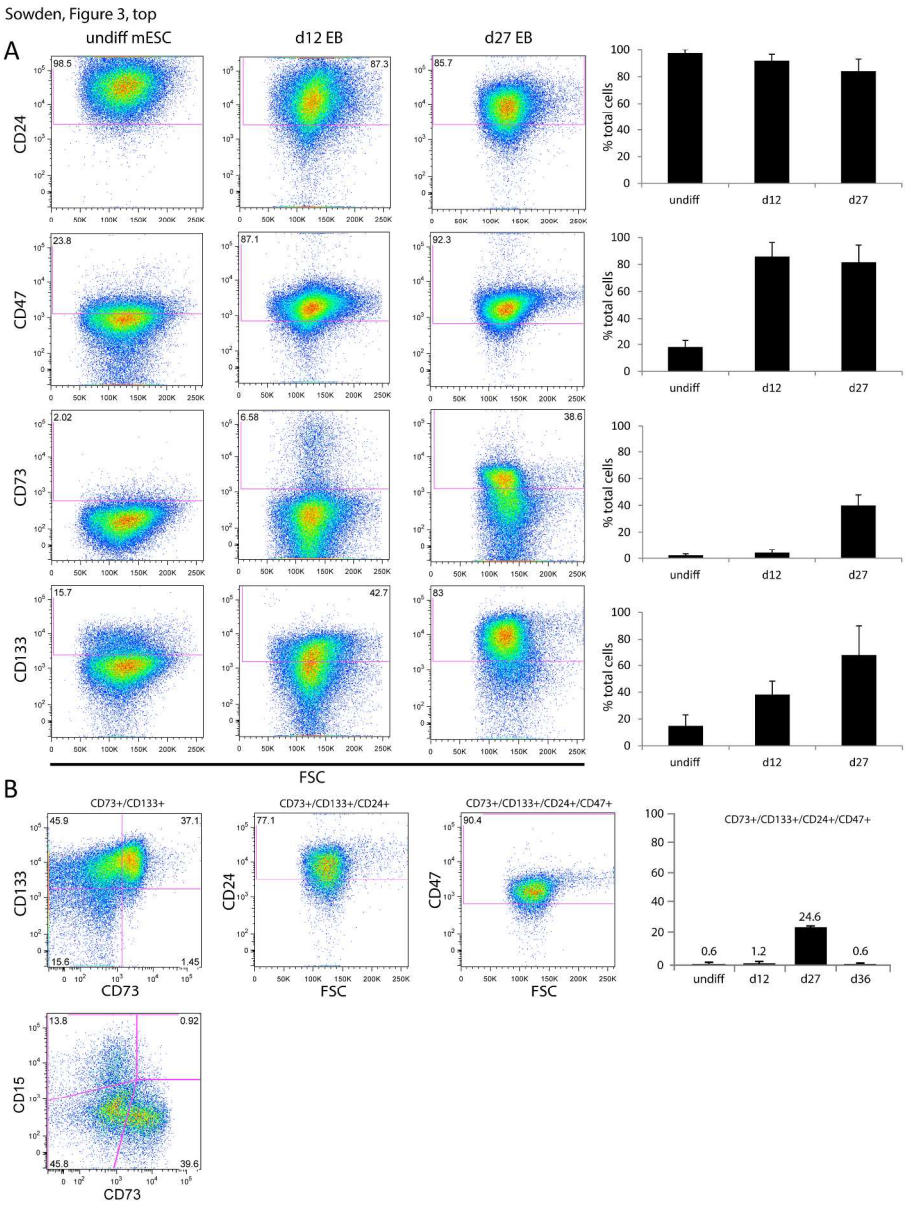

Figure 3 R1
226x302mm (300 x 300 DPI)

Sowden, Figure 4, top

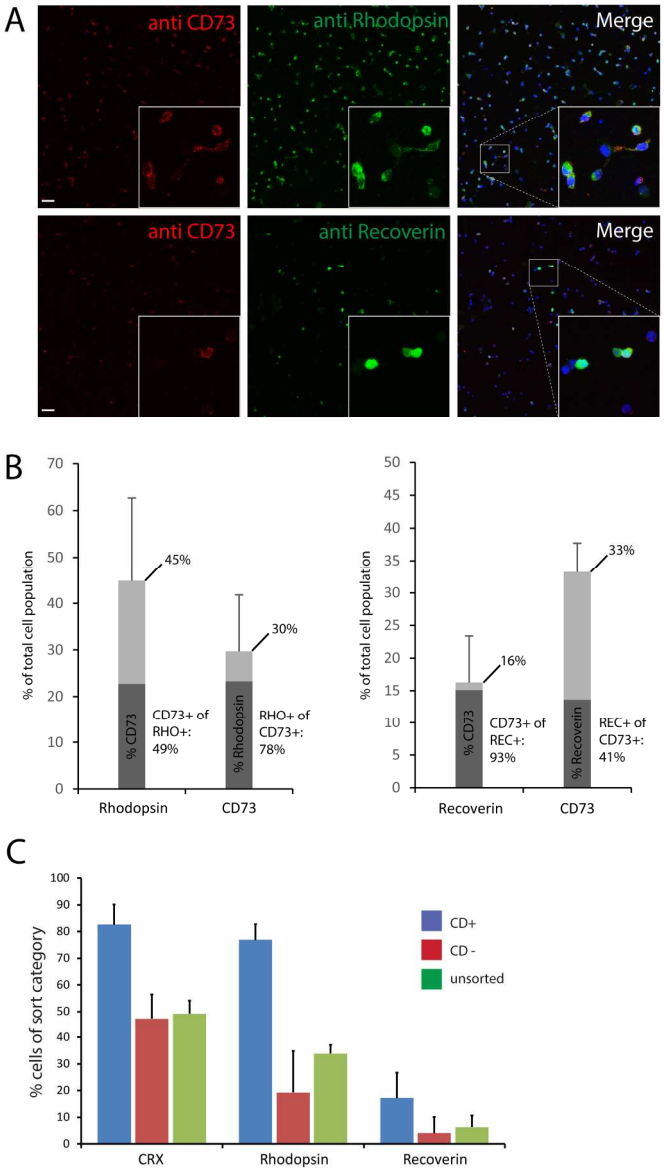

figure 4 R1
130x237mm (300 x 300 DPI)

Sowden, Figure 5, top

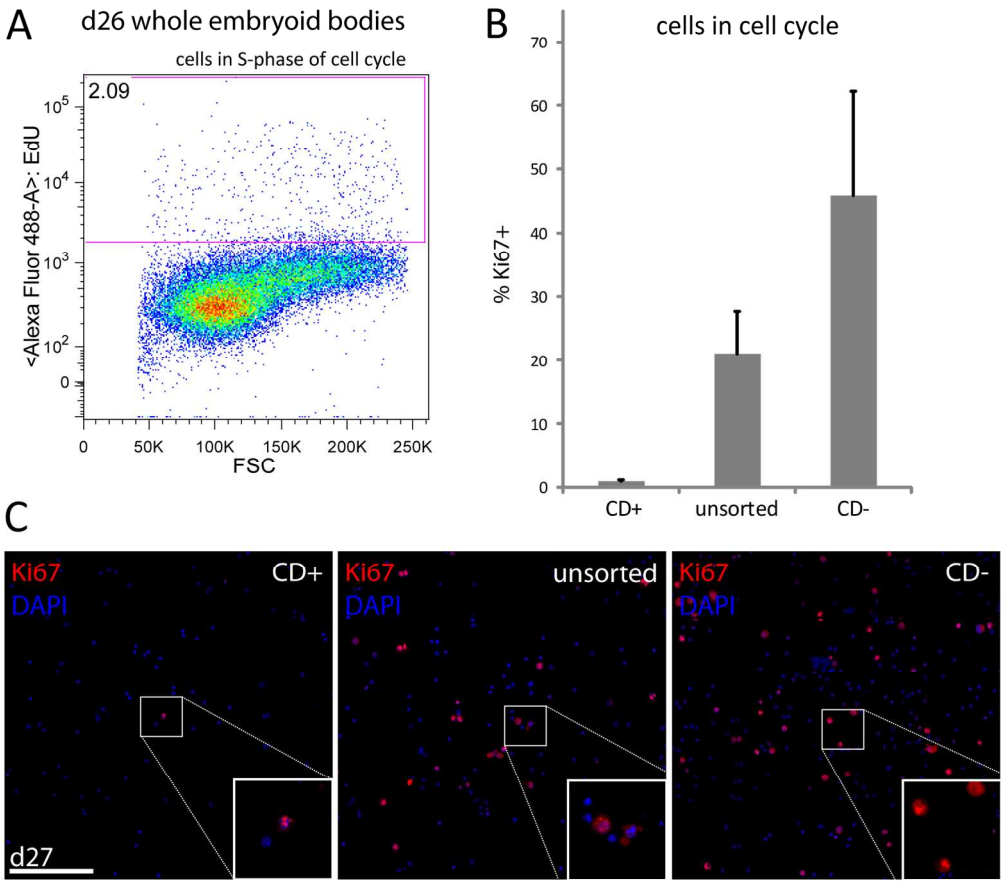

Figure 5
152x143mm (300 x 300 DPI)

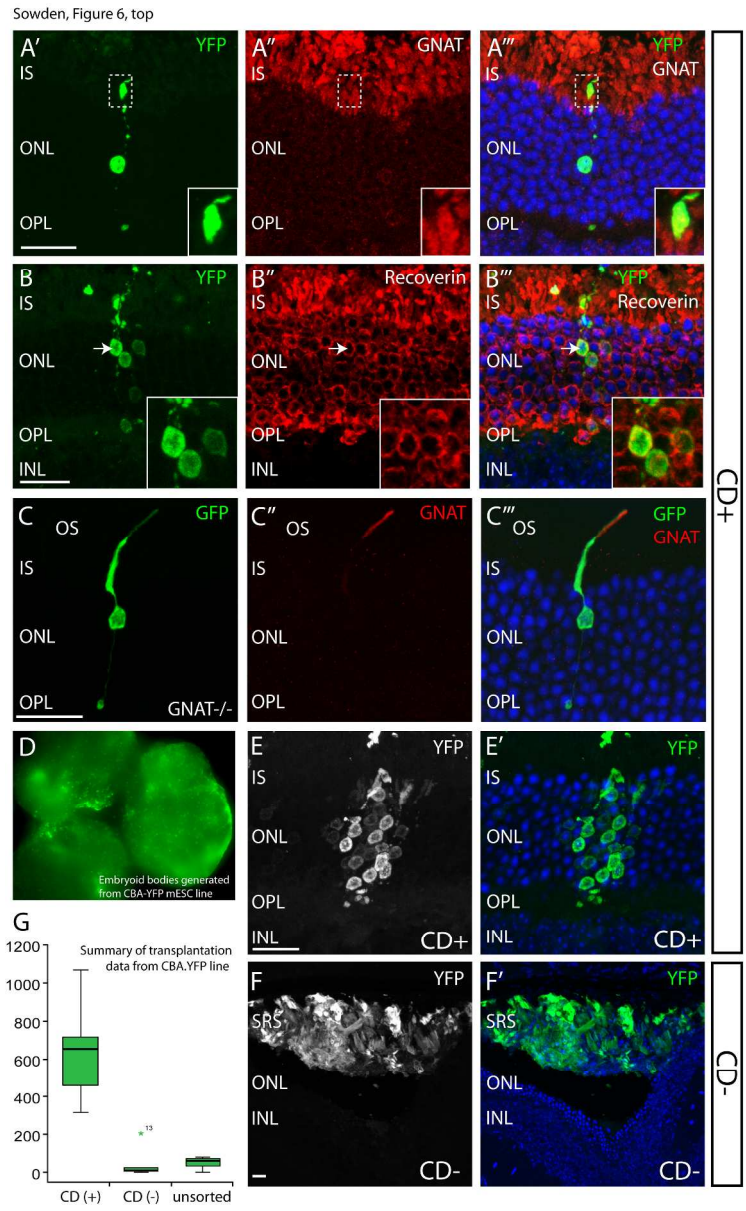

200x326mm (300 x 300 DPI)

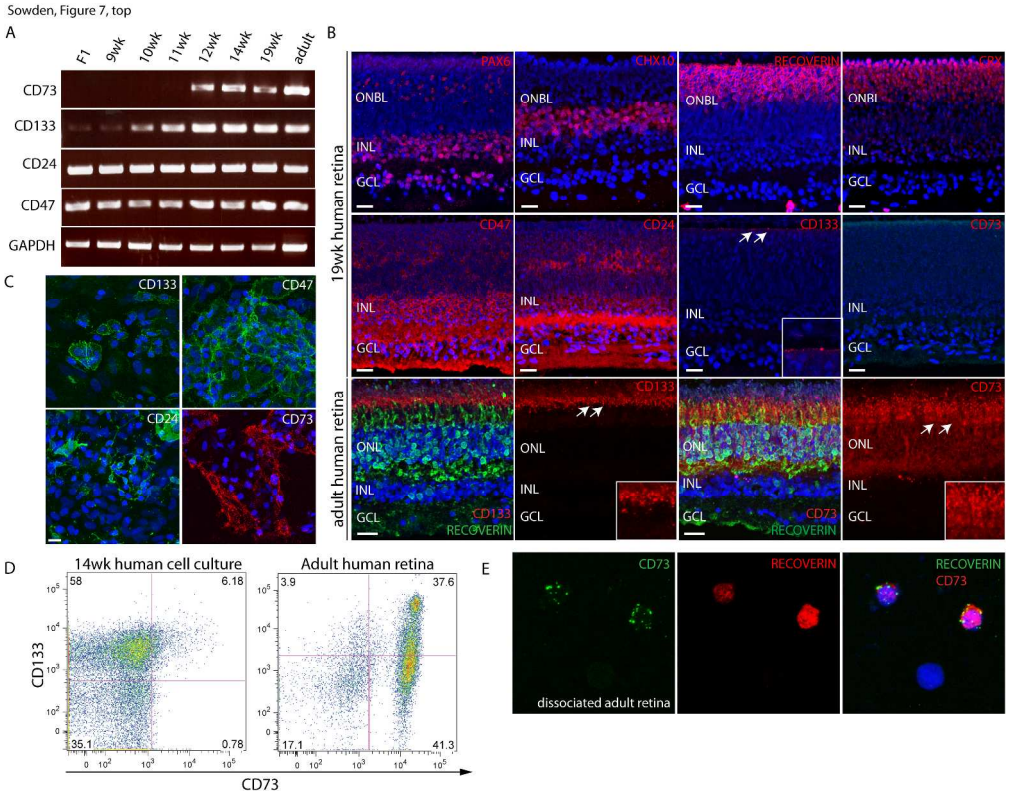

Figure 7
308x242mm (300 x 300 DPI)

Sowden, Supplementary Table 1

enriched in NrlGFP +

Gene name	CD name	log intensity	fold change (+)
Nt5e	CD73	10.5	22.9
Prom1	CD133	10.4	9.2
Lifr	CD118	10.5	6.0
Sema7a	CD108	10.0	5.0
Itga3	CD49c	9.0	3.9
Sirpa	CD172a	10.6	3.7
Cd8a	CD8	6.5	2.2
Jam2	CD322	10.9	2.2
Prnp	CD230	10.3	2.0

enriched in NrlGFP -

Gene name	CD name	log intensity	fold change (-)
Pdgfra	CD140a	9.4	6.5
Kit	CD117	10.3	6.2
Cxcr4	CD184	11.1	5.7
Cd9	CD9	10.2	5.2
Abcg2	CD338	8.2	4.9
Plxnc1	CD232	8.7	4.3
Mcam	CD146	10.2	4.1
Hmmr	CD168	6.5	3.9
Atp1b3	CD298	10.4	3.2
Ngfr	CD271	9.1	3.2
Fgfr1	CD331	8.8	3.0
Cd200	CD200	6.6	2.9
Cd24a	CD24	10.6	2.9
Itga2	CD49b	7.7	2.9
Itgav	CD51	8.8	2.9
Lrp1	CD91	8.1	2.9
Gstm7	CD203c	8.7	2.8
Bmpr1b	CDw293	6.8	2.8
Sema4d	CD100	9.2	2.6
Itgb1	CD29	10.1	2.6
Ddr1	CD167a	10.9	2.4
Ptprj	CD148	7.8	2.4
Il4ra	CD124	7.6	2.1
trf	na	7.1	2.1
Cdh2	na	10.4	2.0

no differential expression

Gene name	CD name	log intensity	fold change (-)
Ace	CD143	5.8	1.3
Adam17	CD156b	8.2	1.3
Alcam	CD166	5.8	1.9
Alk	CD246	5.8	1.5
B3gat1	CD57	7.0	1.9
Bsg	CD147	10.2	1.2
Cd109	CD109	4.9	1.4
Cd151	CD151	6.5	1.9
Cd164	CD164	10.4	1.7
Cd22	CD22	5.1	1.2
Cd247	CD247	5.3	1.2
Cd276	CD276	8.5	1.5
Cd320	CD320	7.5	1.3
Cd37	CD37	6.1	1.4
Cd38	CD38	4.7	1.2
Cd3g	CD3g	4.2	1.2
Cd4	CD4	5.2	1.3
Cd44	CD44	4.8	1.4
Cd47	CD47	9.4	1.4
Cd59a	CD59a	6.7	1.8
Cd68	CD68	6.5	1.3
Cd72	CD72	5.1	1.4
Cd8b1	CD8b1	5.1	1.2
L1cam	CD171	8.5	1.7
Csf1r	CD115	5.1	1.2
Csf2rb	CDw131	5.0	1.3
Entpd1	CD39	5.4	1.2
F11r	na	5.1	1.5
F3	CD142	4.9	1.3
Fasl	CD178	4.7	1.2
Fgfr2	CD332	4.7	1.3
Fgfr3	CD333	7.1	1.6
Fgfr4	CD334	6.0	1.3
Fut4	CD15	5.0	1.2
Gypc	CD236	5.6	1.6
Icam2	CD102	5.8	1.2
Igf1r	CD221	11.0	1.5
Il1r1	CD121a	4.1	1.3
Itga4	CD49D	6.5	1.9
Itga5	CD49e	5.3	1.3
Itga6	CD49f	7.2	1.3
Itgal	CD11a	5.3	1.2
Itgam	CD11b	4.7	1.2
Itgax	CD11c	5.0	1.2
Ly75	CD205	5.7	1.3
Ncam1	CD56	11.1	1.3
Nrp1	CD304	8.0	1.3
Pdgfrb	CD140b	5.5	1.4
Pvrl2	CD112	7.0	1.2
Pvrl3	CD113	8.2	1.3
Sdc1	CD138	6.2	1.3
Siglece	na	5.2	1.2
Tfrc	CD71	9.7	1.4
Thy1	CD90	6.4	1.5
Tlr3	CD283	5.0	1.3
Tnfrsf12a	CD266	7.1	1.6
Tnfrsf17	CD269	5.3	1.2
Tnfsf13b	CD257	5.3	1.2
Tspan7	CD231	12.1	1.6
Vcam1	CD106	5.0	1.4

Supplementary Table 1. CD surface marker analysis from P4 Nrl.GFP microarray. Genes encoding for cluster of differentiation (CD) markers expressed in the postnatal day 4 mouse retina. Genes are grouped according to their enrichment in the rod precursor population (Nrl.GFP+), other retinal cell types (Nrl.GFP-), or ubiquitous expression. The log intensity indicates relative signal strength in the microarray experiment and fold change is given as a measure of enrichment between positive and negative cell populations. A fold change value of 2 was used to delineate the two cell populations. Markers used in PPr biomarker panel are highlighted in green.

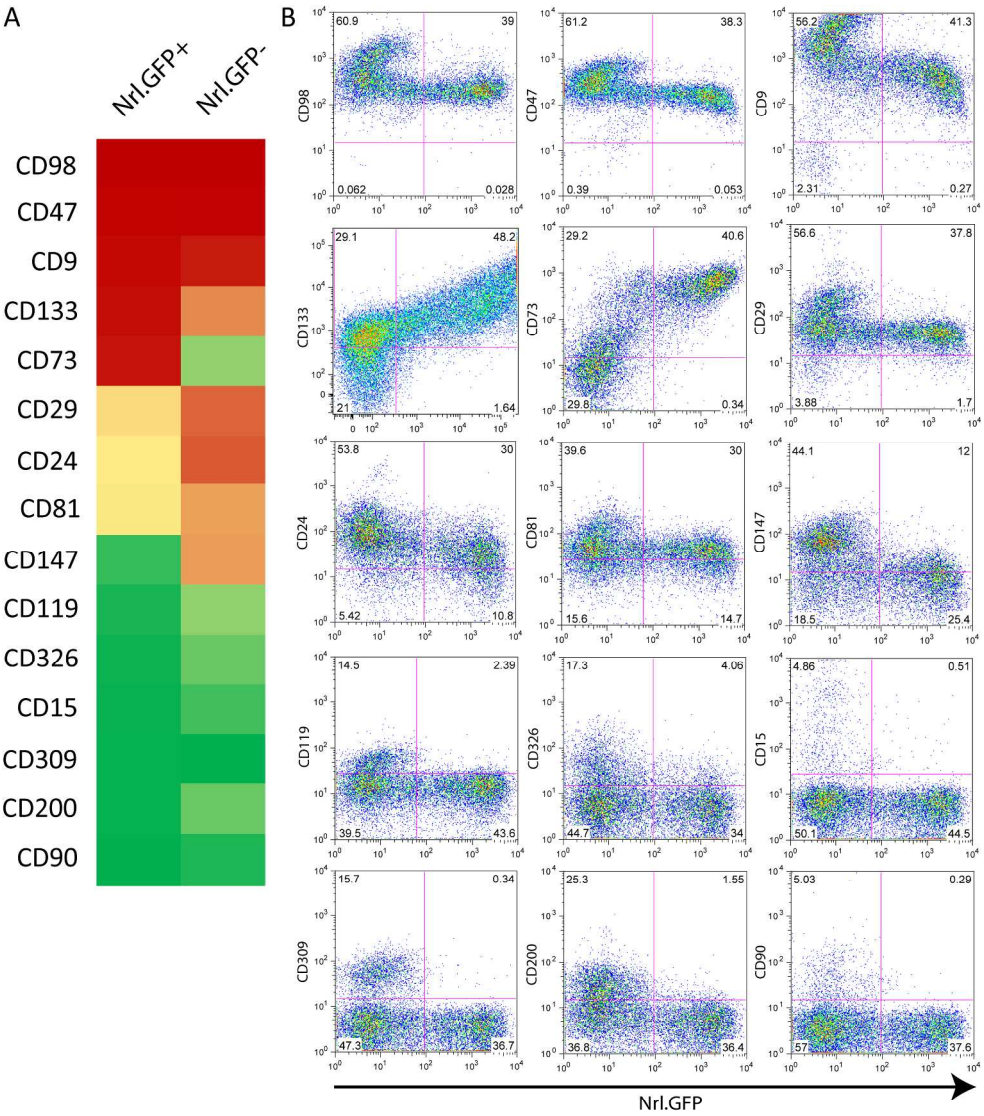

Supplementary figure 1. Cell surface marker screen of P8 Nrl.GFP retinae using BD Lyoplates. (A) Heat map showing top 15 cell surface marker candidates identified in the FACS-based screen. The relative number of cells in the Nrl.GFP positive and Nrl.GFP negative cell populations is indicated (red, high; green, low). (B) Individual flow cytometry scatter plots of dissociated P8 retinal cells for cell surface markers identified in the lyoplate screen. Nrl.GFP intensity is plotted on the x-axis whereas staining intensity of the cell surface markers is shown on the individual y-axes. Top right hand quadrants of scatter plots show CD marker and Nrl.GFP co-labelled cells.

Supplementary Figure 1
233x285mm (300 x 300 DPI)

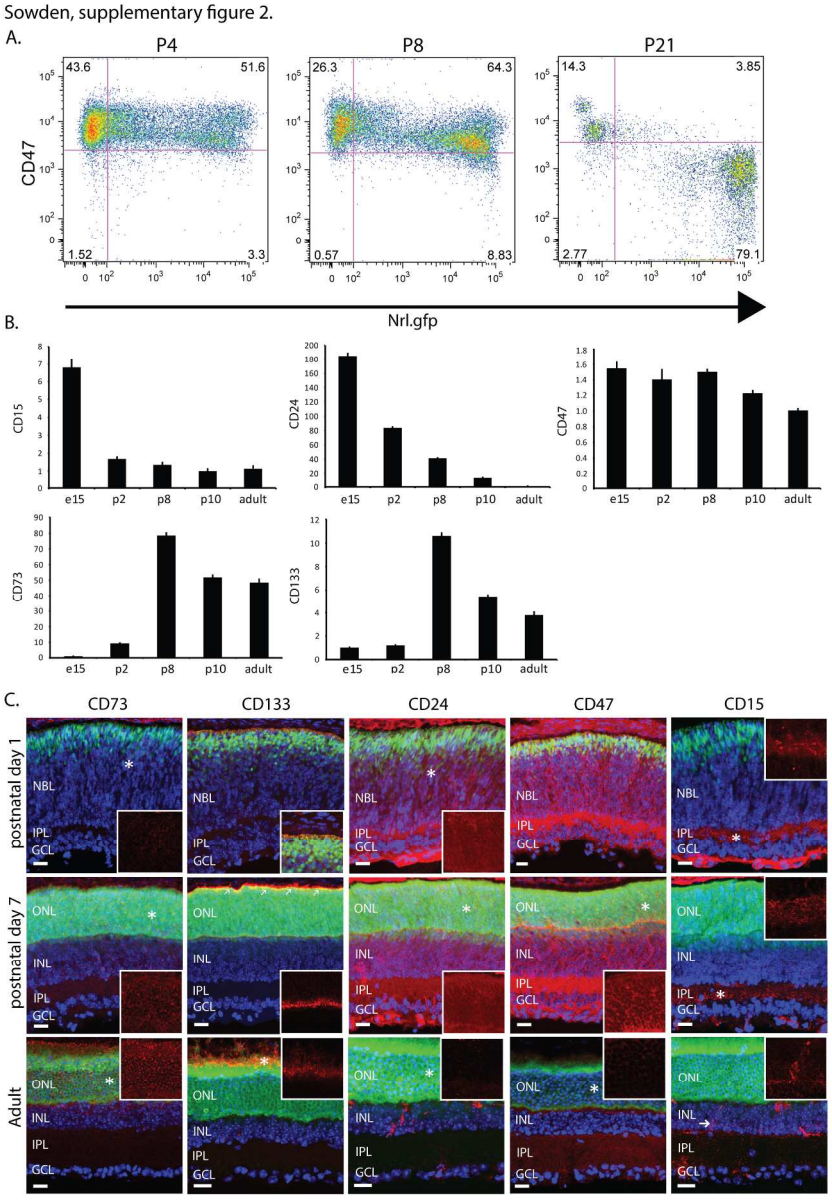

Supplementary Figure 2 R1
179x259mm (300 x 300 DPI)

Supplementary figure 3.

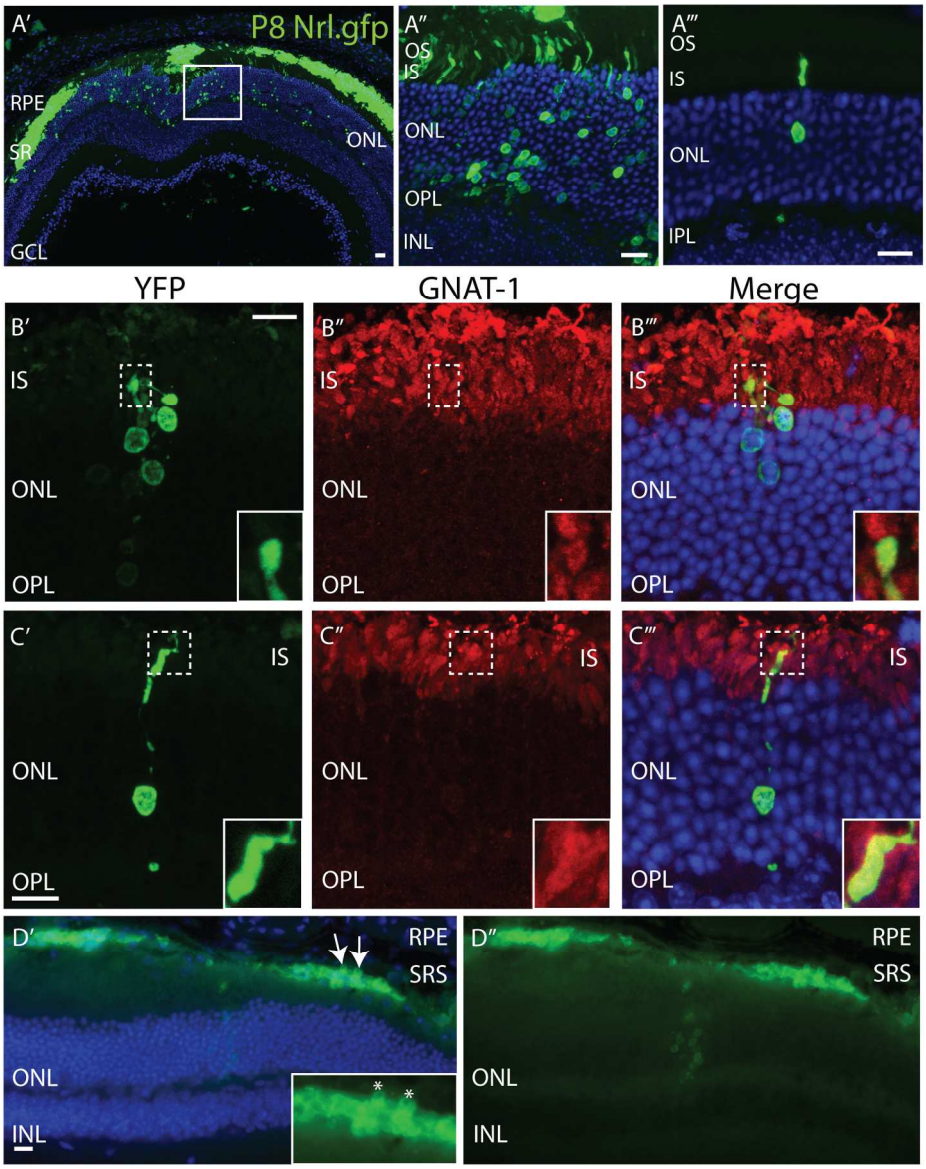

Supplementary Figure 3 R1
154x200mm (300 x 300 DPI)

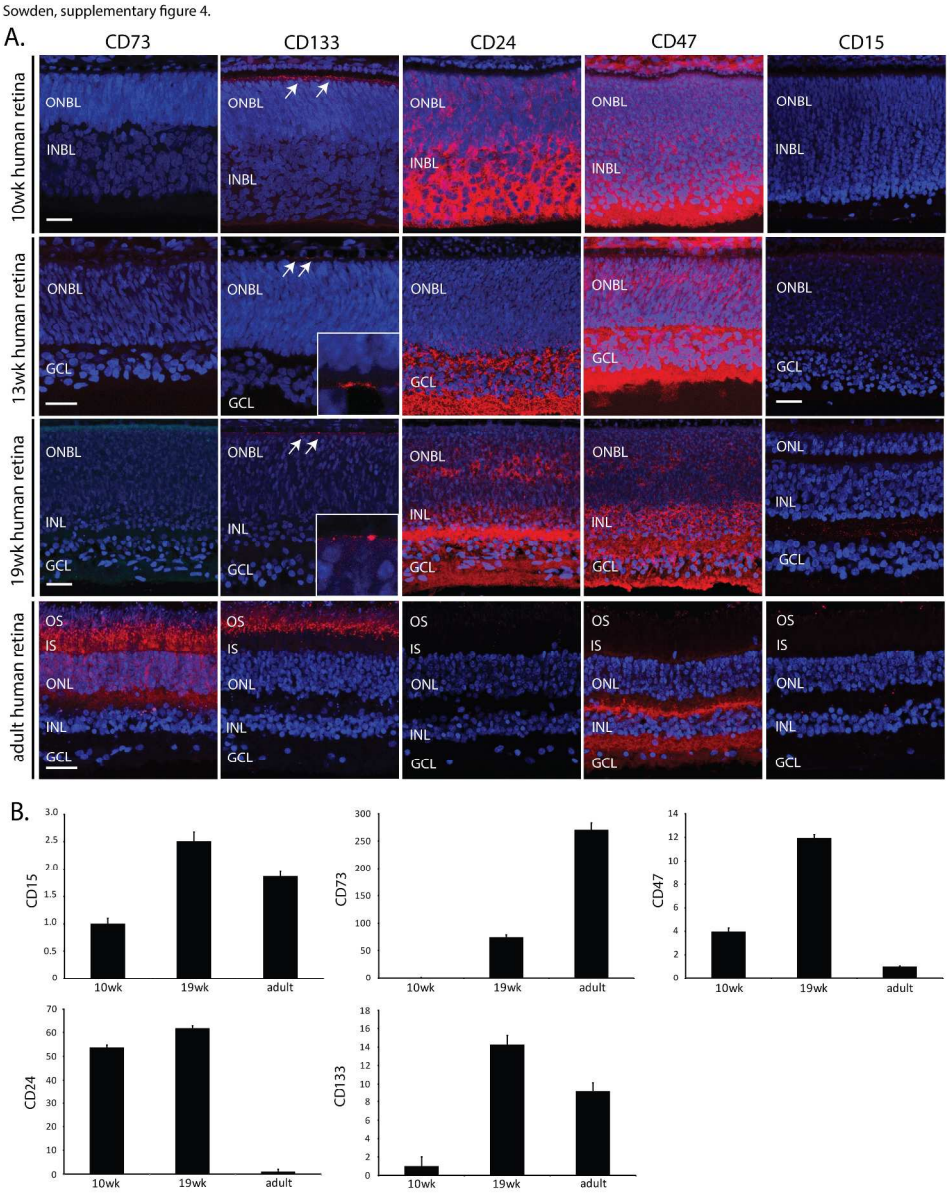

Supplementary Figure 4 R1
269x336mm (300 x 300 DPI)

Supplementary File 1

Material and Methods

Animals

Experimental mice were kept in University College London animal facilities and all experiments were conducted in agreement with the Animals (Scientific Procedures) Act 1986 and the Association for Research in Vision and Ophthalmology Statement for the Use of Animals in Ophthalmic and Vision Research. *C57Bl/6J,* and *Gnat1*$^{-/-}$ (kind gift of J. Lem; [1]) recipient mice were between 6 and 10 weeks of age at the time of transplantation.

Mouse ES cell culture and 3D retinal differentiation

The mouse EK.CCE ESC line [2] (129/SvEv; a kind gift of E. Robertson) or CBA.YFP ESC line (a variant of R1 ESCs; 7AC5/EYFP, from ATCC) were maintained as previously described [3]. On day 0 of retinal differentiation, 3 × 10^4 ESCs were resuspended in one milliliter of differentiation medium (GMEM containing 1.5% KSR, 0.1 mM NEAA, 1 mM pyruvate, 0.1 mM 2-mercaptoethanol) and plated into 96-well low-binding (Corning) plates. Embryoid-body cell aggregates were cultured at 37°C, 5% CO_2 and growth factor-reduced Matrigel (BD Biosciences) was added on day 1 of retinal culture to a final concentration of 2% (v/v). At day 9, whole EBs were transferred into retinal maturation medium (DMEM/F12 Glutamax containing N2 supplement and Pen/strep), plated in low-binding plates at a density of 6 wEBs/cm^2 and maintained at 37 °C, 5% CO_2. The media was changed every

2–3 days and 1 mM taurine (Sigma) and 500 nM retinoic acid (Sigma) were added from day 14 of culture onward.

Histology and Immunohistochemistry

Tissue specimens were fixed in 4% (w/v) phosphate-buffered formaldehyde solution at 4°C for 30min, washed three times with phosphate-buffered saline (PBS) and equilibrated in 30 % (w/v) sucrose solution for cryo-protection at room temperature for 1-2 hours. Subsequently, the specimens were transferred into an optimal cutting temperature (OCT)-compound (RA Lamb) filled mould prior to freezing in a dry ice-methylbutane slurry. Tissue sections were prepared on a cryostat (Leica CM1900 UV) to 14-18 µm thickness and collected onto Superfrost^{TM} plus glass slides (VWR). OCT compound was removed by a 15 min incubation in 37 °C PBS. Tissue sections were then blocked with 10 % (v/v) goat serum, 1 % (w/v) bovine serum albumin (BSA) in PBS containing 0.1 % (v/v) Triton X-100 for one hour at room temperature preceding the primary antibody incubation. Triton X-100 was omitted for staining of cell surface molecules. The following primary antibodies were used; Recoverin, Millipore, 1:1000, overnight, 4°C; Cone arrestin, Millipore, 1:20,000, overnight, 4°C; PKCa, Millipore, 1:1000, overnight, 4°C; Prominin 1, Biolegend, 1:350, overnight, 4°C. CD73 Biolegend 1:250, overnight, 4°C or CD24 BD Bioscience 1:250, overnight, 4°C). The primary antibody was omitted for negative controls. Primary antibody staining was followed by several washes with PBS. Tissue sections were then incubated for 1h at room temperature with the corresponding secondary antibody diluted in blocking solution (Goat anti-rabbit AlexaFluor594, Invitrogen, A-11037, 1:300; Donkey

anti-sheep Cy3, Jackson, 1:500; Goat anti-mouse AlexaFluor594, Invitrogen, 1:500). Hoechst 33342 (1:3000, Sigma-Aldrich) was applied for 10 min at room temperature to visualize nuclei, followed by three several washes with PBS prior to cover-slipping with the Citifluor AF-1 (Electron Microscopy Science) mounting medium.

Dissociation of Retinal Cells/ESC retinal cultures and Flow Cytometry

Neural retinae from wild-type eyes were isolated by micro-dissection and dissociated into a single cell suspension using enzymatic treatment with papain according to the manufacturer's instructions (Worthington Biochemical, Lorne Laboratories, UK). In the case for mouse ESC cultures, differentiated whole embryoid bodies from day 12 and 27 of differentiation were used for analysis and treated similarly to retinal tissue. Eyes from a variety of developmental stages (E15.5, E17.5) and postnatal day, [P] 4, and [P] 8 as well adult were isolated and dissociated.

Following dissociation cells were resuspended in FACS blocking buffer containing 1% BSA (w/v), phosphate-buffered saline and incubated for 45min on ice. The conjugated antibody or IgG isotype controls were added and cells were incubated in the dark on ice for additional 45min. The conjugated monoclonal antibodies were used for FACS analysis: PE-conjugated CD73 (clone TY/11.8, eBioscience); Phycoerythrin-Cy7 conjugated CD24 (clone M1/69, BD Bioscience); PerCP-eFluor710 conjugated Prominin-1 (CD133, clone 13A4, eBioscience); AlexaFluor 647 conjugated CD47 (Biolegend, miap301); V450 conjugated CD15 (clone MC480, BD Horizon). Antibody

specificity for these monoclonal antibodies including Western blot analysis has been previously demonstrated. The same antibody clones were used for FACS and immunohistochemistry analyses. FACS antibodies were used according to manufacturer's instructions.

After staining the cells were centrifuged at 200g for 5min at 4°C and resuspended in PBS and kept on ice until analysis. FACS analysis was carried out using a BD Bioscience LSR II flowcytometer and FlowJo software (Tree Star, USA). FACS gates were set according to specific isotype controls and at least 20000 events of live cells were analysed. FACS compensation was carried out using BD FACSDiva software using single stained controls for each conjugated antibody. Data presented is from at least 3 biological replicates.

Immunocytochemistry on dissociated and FAC-sorted ESC-derived cells

Day 27 ESC retinal cultures were dissociated and sorted via biomarker panel as described above. 50000 cells were plated on poly-lysine/laminin coated coverslips and allowed to adhere for 30min at 37C. Coverslips were then washed once with PBS and adherent cells fixed with 4% PFA/PBS for 10min at room temperature. Following three times washing with PBS, samples were blocking in 10% FBS, 1% BSA/ PBS containing 0.1 % (v/v) Triton X-100 for 1h at room temperature. The blocking solution was replaced by staining solution containing anti-Ki67 antibody in 10% FBS, 1% BSA/ PBS (0.1 % (v/v) Triton X-100). The primary antibody was omitted for negative controls. Finally coverslips with adherent cells were then incubated for 1h at room temperature

with the secondary antibody diluted in blocking solution (Invitrogen, Goat anti-rabbit AlexaFluor594) and counter stained 5min with DAPI. The percentage Ki67 positive cells in the experimental groups was established by Cellprofiler analysis software, using confocal tile scans and was verified by manual cell counts; > 100 cells were counted from 3 biological replicates for each condition.

Microarray and lyoplate and screen for cell surface markers

Postnatal day 4 Nrl.GFP microarray data were previously published [4] and deposited in the National Center for Biotechnology Information's (NCBI; Bethesda, MD) Gene Expression Omnibus (GEO accession number E-MEXP-3922). Array data were further analysed using Onto-express (http://vortex.cs.wayne.edu/ontoexpress/) and DAVID (**D**atabase for **A**nnotation, **V**isualization and **I**ntegrated **D**iscovery; http://david.abcc.ncifcrf.gov/home.jsp), in order to discover genes encoding cell surface CD markers.

Retinal cell suspensions from P8 Nrl.GFP mice were prepared as described above and manufacturers recommendations were followed to conduct the antibody screen using lyoplates (BD). All centrifugation steps were carried out at 300g for 5min at 4°C. After retinal dissociation cells were resuspended in FACS staining buffer (BD) and adjusted to a cell concentration of 10 million cells per 1ml followed by transfer of the cell into round bottom 96-well plates (BD Falcon, Cat. No. 351177). 20 µl of reconstituted primary monoclonal antibody solution was then added to the cells, mixed and incubated on ice for

30 minutes. This was followed by several washing steps with stain buffer (BD Pharmingen) after which the cells were incubated for 30 min with the appropriate biotinylated secondary antibody (rat, 1.25ug/ml; Syrian hamster, 1.25ug/ml; Armenian hamster, 0.6ug/ml; mouse, 1.25ug/ml). Following several washing steps 100 µl of Alexa Fluor® 647 Streptavidin (1:4000, 0.5ug/ml) was added to each well containing cells stained with the biotinylated secondary antibodies and incubated on ice in the dark for 30min. Finally, stained cells were washed several times and analysed on a BD FACSCalibur. At least 30,000 events were collected for the analysis using FACSDiva software and monoclonal antibodies were assessed for their ability to label Nrl.GFP positive rod precursors.

Cell cycle analysis

Click-iT EdU analysis was carried out according to manufacturer's recommendations (Life Technologies). Briefly, whole day 27 embryoid body derived retinal cultures were incubated with 10uM EdU for 2h at 37^0C. Cells were harvested as described above (Dissociation of Retinal Cells/ ESC retinal cultures and Flow Cytometry) and blocked in 1% BSA in PBS. Cells were pelleted and 100ul fixative (4% PFA) was added followed by a 15min incubation at room temperature. The cells were then washed with 1% BSA in PBS, pelleted and re-suspended in 100ul of 1xClick-iT saponin based permeabilization and wash reagent. After 15min of incubation at room temperature 1x Click-iT reaction cocktail was added to the sample and incubated for 30min at room temperature followed resuspension in

wash/permeabilization buffer. FACS analysis was carried out on a BD LSRII using unstained EdU negative cells as a control.

For **Ki67 assay** day 27 ESC retinal cultures were dissociated and sorted via the biomarker panel as described above. 50000 cells were plated on poly-lysine/laminin coated coverslips and allowed to adhere for 30min at 37^{o}C. Coverslips were then washed once with PBS and adherent cells fixed with 4% PFA/PBS for 10min at room temperature. Following three times washing with PBS, samples were placed in blocking solution (10% FBS, 1% BSA/ PBS containing 0.1 % (v/v) Triton X-100) for 1h at room temperature. The blocking solution containing anti-Ki67 antibody was then added for 60 minutes at room temperature. The primary antibody was omitted for negative controls. Finally, coverslips with adherent cells were then incubated for 1h at room temperature with the secondary antibody diluted in blocking solution (Invitrogen, Goat anti-rabbit AlexaFluor594) and counter stained for 5min with DAPI. The percentage Ki67 positive cells in the experimental groups was established by Cellprofiler analysis software, using confocal tile scans and was verified by manual cell counts.

Retinal Cell Transplantations

Donor cells for subretinal transplantation were derived from either CCE or ATCC-R mouse ESC lines, or from Nrl.GFP postnatal day 8 retinae (Nrl.GFP mice were a kind gift of A. Swaroop; [5]), and isolated as described above. For transplantation via PPr biomarkers, cells were incubated in blocking solution (1%BSA/PBS) for 1h and subsequently stained with specific

monoclonal antibodies (see above) directed towards the biomarkers according to manufacturer's recommendations or respective isotype controls. ESC-derived photoreceptor precursors were isolated by FAC-sorting (BD FACS AriaIII) with gating determined for each individual experiment using single stained controls and combined isotype controls. GFP/YFP fluorescence of donor cells was not taken into consideration for cell isolation. Cells in experimental group "unsorted" were processed identically to labelled cells except they were ungated. Post sort cell viability was > 85% based on DAPI staining, and the sorted cells were resuspended at 200,000 live cells/μl in injection buffer (EBSS, DNaseI) after centrifugation at 200g for 10min using a Heraeus Labfuge 400R (Thermos, UK).

Recipient mice (6-8wk, C57Bl/6J or *Gnat1*$^{-/-}$) were anaesthetised with an intraperitoneal injection of 0.2 ml of a mixture of Domitor (1 mg/ml (medetomidine hydrochloride, Pfizer Pharmaceuticals, Kent UK), ketamine (100 mg/ml, Fort Dodge Animal Health, Southampton, UK) and sterile water (ratio 5 : 3 : 42). Topical application of 1% tropicamide was used to dilate pupils of animals and injections were performed using a Zeiss operating microscope. Fundi were visualised using a contact lens system consisting of a coverslip and a drop of coupling medium liquid (Viscotears, Novartis Pharmaceuticals, Frimley, UK). The 34G injection needle loaded with 1 μl of cell suspension (containing 200,000 live FAC-sorted cells) was inserted under direct visualization through the superior equatorial sclera and guided into the sub-retinal space and towards the posterior pole, creating a self-sealing sclerotomy. Injection of the cell suspension in the superior hemisphere

resulted in a bullous retinal detachment around the injection site. Anaesthesia was reversed by administration of 0.2ml of Antisedan (atipamezole hydrochloride 0.10 mg/ml, Pfizer, Kent UK). The retinas of recipient mice were harvested 3 weeks post cell transplantation and processed for analysis.

Counts of integrated photoreceptors

The number of integrated photoreceptor cells in the ONL of recipient retinae was established by counting serial sections of the eye. CBA.YFP cells with a cell body located within the ONL and displaying at least one of the following structures: inner/outer segment, inner/outer processes, synapse in the OPL, were scored as new integrated photoreceptors. The total number of integrated cells per eye was determined by counting all the integrated CBA.YFP+ cells in alternate serial sections through each eye. All transplanted eyes that contained CBA.YFP cells in the ONL and/or the sub retinal space were included in statistical analyses and all data points are represented in graphs. Mann Whitney tests were used to compare median integration efficiencies between samples.

Microscopy, Image Acquisition, and Processing

For epifluorescent analysis retinal sections were viewed on a Zeiss Axioplan 2 and images captured using a Jenoptik C14 digital camera (OpenLab, Improvision). A Zeiss LSM710 (Zen2009, Zeiss) was used for acquisition of confocal micrographs. Images were processed in Zen2009 (Zeiss), Photoshop CS4 (Adobe), Illustrator CS4 (Adobe) and FIJI. Double-labelling analysis was carried out in Adobe Photoshop CS4.

Transcript analysis by quantitative Real-Time Polymerase Chain Reaction (qRT-PCR)

Total RNA was extracted from retinal induced embryoid bodies or from FAC-sorted cell populations using the RNeasy Mini Kit (Qiagen, UK). An on-column DNA digest was performed to eliminate all trace amounts of genomic DNA from the samples. Following quantification of total RNA using a NanoDrop ND-1000 spectrophotometer, cDNA was generated by means of M-MLV-reverse transcriptase (Promega, USA). Gene expression levels were established for *Nt5e*, *Cd24a, Cd47, Cd15* and *Prom1* using Applied Biosystems Taqman PCR reagents and probes on a 7500 Real-Time PCR System according to manufacturer's recommendations. Gene expression data was normalized using Gapdh as a reference. The mean RQ values as well as RQmin and RQmax as measures of variation were calculated using ABI 7500 software 2.0.1.

Human retinal cultures

Human fetal retinal tissue was micro-dissected and dissociated using a papain solution according to manufacturer's recommendation (Worthington Biochemical Corporation, Lorne Laboratories, UK). Cells were seeded on poly-L-lysine (Sigma-Aldrich) and laminin (Sigma-Aldrich, 1mg/ml) coated glass coverslips and cultured in retinal differentiation media containing DMEM-F12 Glutamax (Invitrogen), 1 x N2 and 1 x B27 neural supplements (Invitrogen) and 10% FBS (Invitrogen) as well as penicillin/streptomycin (Invitrogen). Cell culture media was changed every 2-3 days.

Reference List

1. Calvert PD, Krasnoperova NV, Lyubarsky AL et al. Phototransduction in transgenic mice after targeted deletion of the rod transducin alpha - subunit. **Proc Natl Acad Sci U S A**. 2000;97:13913-13918.
2. Evans MJ, Kaufman MH. Establishment in culture of pluripotential cells from mouse embryos. **Nature**. 1981;292:154-156.
3. Osakada F, Ikeda H, Mandai M et al. Toward the generation of rod and cone photoreceptors from mouse, monkey and human embryonic stem cells. **Nat Biotechnol**. 2008;26:215-224.
4. Lakowski J, Han YT, Pearson RA et al. Effective transplantation of photoreceptor precursor cells selected via cell surface antigen expression. **Stem Cells**. 2011;29:1391-1404.
5. Akimoto M, Cheng H, Zhu D et al. Targeting of GFP to newborn rods by Nrl promoter and temporal expression profiling of flow-sorted photoreceptors. **Proc Natl Acad Sci U S A**. 2006;103:3890-3895.